EFFECT OF PRE-AGEING CONDITIONS ON THE HARDNESS AND CORROSION CHARACTERISTICS OF DOUBLE-THERMALLY AGED Al-Si-Mg ALLOY

By

Bello Okatengwu UMARU, B.ENG (A.B.U) 2009
MSc/Eng/01429/10-11

A THESIS SUBMITTED TO THE SCHOOL OF POSTGRADUATE STUDIES,
AHMADU BELLO UNIVERSITY, ZARIA

IN PARTIAL FULFILMENT OF THE REQUIREMENTS FOR THE AWARD
OF A
MASTER DEGREE IN METALLURGICAL AND MATERIALS ENGINEERING.

DEPARTMENT OF METALLURGICAL AND MATERIALS ENGINEERING,
FACULTY OF ENGINEERING
AHMADU BELLO UNIVERSITY, ZARIA
NIGERIA

MARCH 2013

Declaration

I declare that the work in this Thesis entitled "The effect of Pre-ageing Conditions on the Hardness and Corrosion Characteristics of Double-Thermally Aged Al-Si-Mg alloy" has been carried out by me in the Department of Metallurgical and Materials Engineering. The information derived from the literature has been duly acknowledged in the text and a list of references provided. No part of this thesis was previously presented for another degree or diploma at this or any other Institution.

Name of Student	Signature	Date

Certification

This thesis entitled "EFFECT OF PRE-AGEING CONDITIONS ON THE HARDNESS AND CORROSION CHARACTERISTICS OF DOUBLE-THERMALLY AGED Al-Si-Mg ALLOY" by BELLO OKATENGWU UMARU meets the regulations governing the award of the degree of Masters of Science of the Ahmadu Bello University, and is approved for its contribution to knowledge and literary presentation.

_____ Date_____

Dr. M. Abdulwahab
Chairman, Supervisory Committee

_____ Date_____

Prof. S. A. Yaro
Member, Supervisory Committee

_____ Date_____

Prof. S. A. Yaro
Head of Department

_____ Date_____

Prof. A. A. Joshua
Dean, School of Postgraduate Studies

Acknowledgements

In the name of ALLAH the most Gracious, the most Merciful, the Praise Worthy, all thanks are due to him, the Lord of the heavens and the universe, who made everything possible and easier for me, may His Peace and Blessings be upon His messenger Prophet Muhammad (S. A. W).

I would like to register my appreciation to my supervisors Dr. M. Abdulwahab and Professor S. A. Yaro for being very accommodating at my unscheduled consultation hours and for their positive critisms and suggestions. To this I would say JazaKallahu Khairan. I also appreciate the help of all academic and non-academic staff of the department for their supports towards the success of this thesis.

My sincere and special thanks go to my beloved parent Alhaji and Hajiya M. J. Umaru for their guidance, love, encouragement, prayers and financial supports towards the achievement of this academic programme. So also are my brothers and sisters. I remain indebted to them all may Allah reward your efforts abundantly and grant you all your heart desires.

Finally my regards to my friends and all my class members who have contributed either directly or indirectly to the success of this thesis, but for which time and space cannot permit me to write their names.

Abstract

The effect of pre-ageing condition on the hardness and corrosion characteristics of double-thermally aged treatment (DTAT) chill cast Al-Si-Mg alloys in simulated seawater environment using elemental sodium-modifier has been studied. This was with a view to improving the precipitation response and corrosion resistance of the Al-Si-Mg alloy. The temper conditions are DTAT at 90^{o}C, 105^{o}C and 120^{o}C with variable pre-ageing time 1-5 h respectively. These were compared with the as-cast and single thermally aged (STA) treated samples. The hardness of the Al-Si-Mg alloy was determined using the Rockwell-F scale hardness tester, while the corrosion characteristics was evaluated using weight loss and linear polarisation corrosion techniques in 3.5% NaCl solution. Within the α-aluminium solid solution, the elements are indicated by the Energy Dispersive Spectrum (EDS). From the results DTAT samples showed better hardness values as compared with the STAT and as-cast samples. The DTA treatment produced increased hardness value of the samples more than 100%. These significant improvements were evidenced in the DTAT at 120^{o}C for 3 h (with a hardness value of 18.2 HRF) and DTAT at 120^{o}C for 4 h (with a hardness value of 9.8 HRF). Improvement in the hardness can be attributed to fine coherent clusters precipitates which serve as obstacle to dislocation movement. The corrosion of the DTAT samples in all temper conditions in the simulated seawater showed a higher improvement in corrosion resistance than the as-cast and conventional STAT alloy. From the Optical Microscope (OPM) results of as-corroded samples, it is obvious that the type of corrosion that occurred in this alloy is pitting/uniform corrosion. The hardness results of some selected samples after weight loss corrosion in simulated seawater

also showed a decrease in hardness value as compared with its hardness before corrosion attack. The linear polarisation of some of the thermally treated samples demonstrated a higher corrosion potential and linear polarisation resistance with lower current density compared to the as-cast and STAT samples. It can be deduced that the thermal treatment have improved the hardness and corrosion resistance of the alloy under the studied condition.

Table of Contents

Page

Title page ……..…….....i

Declaration ii

Certification..... iii

Acknowledgements.....iv

Abstract v

Table of Contents.....vii

List of Figures.....x

List of Plates xi

List of Tables.....xii

List of Abbreviations, Notations and Units.....xiii

INTRODUCTION 1

1.1 Statement of Research Problem.....2

1.2 Aims and Objectives 2

1.3 Justification of the Research.....3

1.4 Scope of Work 4

1.5 Contribution to Knowledge 4

LITERATURE REVIEW.....5

2.1 Introduction 5

2.2 Aluminium alloy 6

2.2.1 Classification of Aluminium Alloy.....6

2.2.2 Aluminium Cast Alloy Designations 7

2.3Al-Si Foundary Alloys 8

2.4 Ternary diagram in Al-Si-Mg alloy 11

2.5 Al-Si-Mg alloys 13

2.6 Heat Treatment 0f Cast Al-Si-Mg alloys 13

2.6.1 Effect of Solutionizing Temperature and time on Al-Si-Mg alloy 14

2.6.2 Effect of quenching rate 15
2.6.3 Effect of ageing time and temperature 16
2.7 Hardness Measurement of Al-Si-Mg alloy 17
2.7.1 Rockwell hardness test 18
2.8 Microstructure of Al-Si-Mg alloy 18
2.9 Mechanical Properties of Al-Si-Mg alloy 19
2.10 Pre-ageing/interrupted ageing treatment in Al-Si-Mg alloy 20
2.11 Corrosion Properties of aluminium alloys 20
2.12.1 Direct Method 21
2.12.1.1 Visual/Optical Measurement 21
2.12.1.2 Weight loss of coupon 21
2.12.2 Linear polarization resistance (LPR) 22
2.12.3 Electrical Resistance (ER) Equipment 22
2.13 Mechanism of electrochemical corrosion 23
2.14 Forms of corrosion 24
2.14.1 Uniform Attack 24
2.14.2 Pitting 25
2.14.3 Intergranular Corrosion 25
2.14.4 Stress Corrosion 26
2.15 Applications of Aluminium and its alloys 28
MATERIALS AND METHOD 30
3.1 Materials and equipment 30
3.1.1 Materials 30
3.1.2 Equipment 30
3.2 Methods 31
3.2.1 Casting of the samples 31
3.2.2 Heat treatment of the Al-Si-Mg alloy 31
3.2.2.1 Double Thermal Ageing Treatment (DTAT) 32
3.2.3 Hardness measurement 32

3.2.4 Electrochemical Corrosion Technique 33
3.2.4.1 Weight loss 33
3.2.4.1.1 Corrosion Rate Determination 33
3.2.4.2 Linear Polarisation corrosion study 34
3.2.4.3 Linear Polarisation corrosion Measurement 35
3.2.5 Microstructural examination 37
RESULTS AND DISCUSSION 38
4.1 RESULTS 38
4.2 Discussion 47
4.2.1.2 Double Thermal Ageing (DTAT)-T7 treatment 48
4.2.1.3: Comparative study between DTAT, STAT and as-cast Al-Si-Mg alloy studied 52
4.2.2 Correlation between Microstructures, Hardness and Corrosion Characteristics of Al-Si-Mg alloys 52
4.2.3 CORROSION CHARACTERISTICS AND THERMAL AGEING TREATMENT 56
4.2.3.1 Weight loss 56
4.2.3.2 Linear Polarisation Corrosion 60
SUMMARY, CONCLUSION AND RECOMMENDATIONS 67
5.1 Summary 67
5.2 Conclusion 68
5.3 RECOMMENDATIONS FOR FURTHER WORKS 70
REFERENCES 71

List of Figures

Page

Figure 2.1: Al-Si cast alloy phase diagram (Jacobs, 1999)……10
Figure 2.2: Representation of ternary composition.....12
Figure 2.3: Ternary phase diagram for a composition base for an ABC.....12
Figure3.1: Schematic diagram of the DTAT heat treatment cycle indicating Pre-ageing regions……32
Figure 4.1: Hardness of Al-Si-Mg alloy under different condition of ageing……....47
Figure 4.2: Variation of hardness with ageing time of Al-Si-Mg alloy after DTAT at 90^{o}C……...49
Figure 4.3: Variation of hardness with ageing time of Al-Si-Mg alloy after DTAT at 105^{o}C……...49
Figure 4.4: Variation of hardness with ageing time of Al-Si-Mg alloy after DTAT at 120^{o}C……...50
Figure 4.5: Corrosion characteristics of Al-Si-Mg alloy under different condition of ageing with the as-cast…….56
Figure 4.6: Variation of corrosion rate with ageing time for DTAT at 90^{o}C…….57
Figure 4.7: Variation of corrosion rate with ageing time for DTAT at 105^{o}C……...57
Figure 4.8: Variation of corrosion rate with ageing time for DTAT at 120^{o}C……...58
Figure 4.9: Linear Polarisation of as-cast, STAT and DTAT Al-Si-Mg alloy after Pre-ageing at 90^{o}C.....61
Figure 4.10: Linear Polarisation of as-cast, STAT and DTAT Al-Si-Mg alloy after Pre-ageing at 105^{o}C……...62
Figure 4.11: Linear Polarisation of as-cast, STAT and DTAT Al-Si-Mg alloy after Pre-ageing at 120^{o}C……..62

List of Plates

Page

Plate 1: SEM microstructure and EDS spectrum of Al-Si-Mg alloy after pre-ageing at 90^{o}C for 3 h.....53

Plate 2: SEM microstructure and EDS spectrum of Al-Si-Mg alloy after pre-ageing at 120^{o}C for 3 h.....54

Plate 3: SEM microstructure and EDS spectrum as-cast of Al-Si-Mg alloy 54

Plate4: SEM microstructure and EDS spectrum of Al-Si-Mg alloy after STAT-T6 treatment at 180^{o}C for 2 h.....55

Plate 5a: Microstructure of unmodified Al-Si-Mg alloy showing silicon flakes within aluminium matrix.....63

Plate 5b: Microstructure of elemental sodium modified Al-Si-Mg alloy showing the breakdown/spheroidization of silicon flakes.....64

Plate 6a: As-corroded microstructure of DTAT 90/3 h Al-Si-Mg alloy after 30 days of immersion in simulated sea water (x300).....64

Plate 6b: As-corroded microstructure of DTAT 105/3 h Al-Si-Mg alloy after 30 days of immersion in simulated sea water (x300).....65

Plate 6c: As-corroded microstructure of DTAT 120/3 h Al-Si-Mg alloy after 30 days of immersion in simulated sea water (x300).....65

Plate 6d: As-corroded microstructure of STAT 180/3 h Al-Si-Mg alloy after 30 days of immersion in simulated sea water (x300).....66

Plate 6e: As-corroded microstructure of as-cast Al-Si-Mg alloy after 30 days of immersion in simulated sea water (x300).....66

List of Tables

Page

Table 2.1: Aluminium Alloy classification system…….....7

Table 2.2: Methods for corrosion measurement…….....22

Table 3.1: Charge calculation of the Al-Si-Mg alloy produced (wt%)…….....31

Table 4.1: Hardness value of Al-Si-Mg alloy after DTAT at 90^{o}C…….....39

Table 4.2: Hardness value of Al-Si-Mg alloy after DTAT at 105^{o}C…….....39

Table 4.3: Hardness value of Al-Si-Mg alloy after DTAT at 120^{o}C…….....40

Table 4.4: Comparism of peak ageing time for DTAT at different ageing temperatures and STAT Al-Si-Mg alloy…….....40

Table 4.5: Comparism of peak hardness for DTAT at different ageing temperatures, STAT and as-cast Al-Si-Mg alloy…….....41

Table 4.6: Comparative study of corrosion rate from weight loss in simulated sea water after 40 days for DTAT-T7, STAT-T6 and as-cast Al-Si-Mg alloy……..42

Table 4.7: Hardness values of some selected Al-Si-Mg alloys after exposure to weight loss corrosion study…….....43

Table 4.8: Comparative study on Linear Polarisation Corrosion data obtained for as-cast, STAT and DTAT Al-Si-Mg alloy in simulated seawater environment after pre-ageing at 90^{o}C…….....44

Table 4.9: Comparative study on Linear Polarisation Corrosion data obtained for as-cast, STAT and DTAT Al-Si-Mg alloy in simulated seawater environment after pre-ageing at 105^{o}C…….....45

Table 4.10: Comparative study on Linear Polarisation Corrosion data obtained for as-cast, STAT and DTAT Al-Si-Mg in simulated seawater environment after pre-ageing at 120^{o}C…….46

List of Abbreviations, Notations and Units

DTAT – This is the T7 temper which involves solution heat treatment and slow precipitation for lower time combined with ageing for stabilization; Solution heat treated + Pre-ageing at temperatures of 90, 105, and 120^{o}C for 1-5 h each + artificial ageing at 180^{o}C/2 h.

STAT – T6 temper which involves solution heat treatment with conventional ageing; Solution heat treatment + artificial ageing at 180^{o}C/2 h.

SHT – Solution heat treatment

HRF – Rockwell micro-hardness number

K – Kelvin (^{o}C + 273)

Sec – Seconds

h – Hour

kgf – A force equal to one kilogram

mm – Millimeter

mpy – mils per year

Ys – Yield strength

Mpa – Mega Pascal (10^{6} Pa)

XRD – X-Ray Diffraction

SEM-EDS – Scanning Electron Microscopy Equipped with Energy Dispersive Spectroscopy

OPM – Optical Microscopy

F- Temper – As-cast alloy

Al-Si-Mg alloy – Aluminium + Silicon + Magnesium alloy

CHAPTER ONE

INTRODUCTION

Aluminium metal is alloyed with elements like Mg, Si, Cu, Mn, Fe and Zn to produce a variety of wrought products for beverage cans to aircraft structural parts, to cast products like engine blocks and steering knuckles for automobiles (Hassan and Aigbodion, 2009). The alloys produced have achieved wide usage in automobile, aerospace and other applications because of their high strength to weight ratio and good corrosion resistance (Kumar *et al*, 2007; Li *et al*, 2006; Zhen, 1997; Sun *et al*, 1999).

Al-Si-Mg alloy is a group of heat treatable cast Al-Si alloys which exhibit good castability and corrosion resistance (Kumar *et al*, 2007). However, the pursuit of high quality castings with consistent mechanical properties depend upon the proper processing of the alloy, including grain refinement, modification and precipitation heat treatment (Kumar *et al*, 2007).

Silicon imparts to Al-Si-Mg alloy good fluidity, resistance to hot cracking and thermal expansion, while magnesium improves its strength-to-weight ratio and yield stress by combining with silicon to form the age-hardening phase (Mg_2Si) which precipitates from a supersaturated solid solution during heat treatment (Birol, 2009).

The addition of alloying elements to aluminium improves its mechanical properties but its corrosion resistance may sometimes be reduced due to precipitation of these elements along the grain boundaries after ageing (Abdulwahab, 2011; Wang *et al*, 2007). Though certain alloying elements can simultaneously improve strength and corrosion resistance (Abdulwahab, 2007).

1.1 Statement of Research Problem

The disadvantages of Al-Si-Mg alloy are its low elastic modulus and precipitation hardening response/ behaviour in the T6 temper; Solution Heat Treatment (SHT) and artificial ageing conditions (Leo and Cerri, 2003; Abdulwahab, 2011).Experiments have shown that ageing for a sufficient time at temperature above about 150^{o}C significantly increase the resistance to corrosion, but reduced strength/hardness in the T6 temper condition of some aluminium alloys as a result of coarsening of precipitates (Abdulwahab, 2011; Wang *et al*, 2009).

One-step ageing (Single Thermal Ageing Treatment; STAT-T6) of aluminium alloys has been reported in several studies concerning Al-Si-Mg alloy in the T6 temper condition (SHT + artificial ageing) (Leo and Cerri, 2003; Haghshenas *et al*, 2008b; Zhang *et al*, 2005; Haghshenas *et al*, 2008). For the purpose of this study a two step ageing (Double Thermal Ageing Treatment; DTAT-T7) was developed for A356.0-type Al-Si-Mg alloy. The T7 temper has been defined in this research as alloy that has undergone solution heat treatment, a variation in the pre-ageing temperature and time with ageing for stabilization.

1.2 Aims and Objectives

The present study was aimed at investigating the effect of double thermal ageing treatment on the hardness and corrosion characteristics of Al-Si-Mg alloy in simulated seawater environment. To achieve this aim, the following specific objectives were pursued.

1. To produce A356.0 type Al-Si-Mg alloy and subject the alloy to STAT, DTAT temper with variable pre-ageing temperatures and times.
2. To study the hardness of the thermally treated and as-cast samples.
3. To investigate the corrosion characteristics of the alloys after thermal ageing using weight loss and electrochemical corrosion method in simulated seawater environment.
4. To study the microstructure of the thermally treated alloys and as-cast with OPM/SEM-EDS respectively.
5. To correlate microstructural changes with corrosion characteristics.

1.3 Justification of the Research

The final properties of an alloy are not due only to its chemical composition, but also to its metallurgical history. It is possible to use lot of different treatments so as to change the properties of an alloy. Thus, finding the optimal treatment conditions is of fundamental importance in achieving the desired properties (Fracasso, 2010). The Al-Si-Mg alloy offer hardening possibilities that leads to specific properties and applications in automobile, aerospace and marine industries. Since precipitation hardening has been outlined as one of the major treatments that are mostly used for the purpose of increasing strength/hardness in aluminium alloys (Abdulwahab, 2011; Birol, 2009; Juang and Wu, 2008) methods for enhancing this treatment remained top research focus in order to make the alloy competitive in future applications.

1.4 Scope of Work

The scope of this research work covers; production of sodium modified Al-Si-Mg alloy through chill casting method, artificial ageing/double thermal ageing treatment with variable pre-ageing temperature and time of the produced alloy, hardness measurement (HRF), corrosion characteristics and microstructure characterization of the alloys. The microstructures were examined using OPM and SEM-EDS.

1.5 Contribution to Knowledge

To the best of my knowledge, no previous work on the variable effect of pre-ageing thermal condition under double-thermal ageing treatment of sodium-modified Al-Si-Mg alloy have been reported. The hardness value and corrosion resistance of the STAT-T6 were enhanced via varying pre-ageing temperature and time of the Al-Si-Mg alloy studied.

CHAPTER TWO

LITERATURE REVIEW

2.1 Introduction

Cast Al-Si-Mg alloys have been widely used in automotive and aircraft industries for their good properties and high strength-to-weight ratio (Ma, 2006). Some of their attractive properties are good extrudability, relative high strength, good corrosion resistance, excellent casting characteristics, light weight and acceptable cost (Lozano and Voort, 2010; Svenningsen, 2006; Wei *et al*, 2005). An intensive study of this cast aluminium family has been found in the literature in terms of enhancing the mechanical properties (Ma, 2006). It is well known that heat treatment is one of the important methods for improving the mechanical properties of aluminium alloys. The heat treatment of the age-hardenable aluminium alloys involves solutionizing the alloys, quenching, and either ageing at room temperature (natural ageing) or at elevated temperature (artificial ageing) (Ma *et al*, 2006).

Generally, the mechanical and microstructural properties of aluminium cast alloys are dependent on the composition, melt treatment conditions, solidification rate, casting process and the applied thermal treatment (Seifeddine, 2007). The mechanical properties of Al-Si-Mg alloys depend, on the distribution and shape of silicon particles rather than of magnesium content. Alloys in which the silicon particles (eutectic or primary) are small, round and evenly distributed are usually highly ductile, while those in which the silicon

particles are faceted and acicular are usually much less ductile but exhibit slightly higher strength (Seifeddine, 2007).

2.2 Aluminium alloy

Aluminium alloys are alloys in which aluminium (Al) is the predominant metal (international Aluminium institute; 2008). The typical alloying elements added to aluminium are Zinc, Magnesium, Copper, Silicon, Iron, Lithium, Manganese, Nickel, Argon, Tin and Titanium (Rashid, 2010). Because of their varying solid solubilities, some are used as solid solution strengtheners, while others are added to form various desirable intermetallic compounds (Rashid, 2010).

2.2.1 Classification of Aluminium Alloy

Most commercial Aluminium alloys belong to one of two families (i) wrought alloys and (ii) casting (or foundry) alloys (Joseph, 2009 and Choundary, 2007).

Wrought alloys are cast into billets and then mechanically worked into their final shape by forging, extrusion, rolling, or drawing. The chemical composition of wrought alloys is tailored to provide the material with sufficient ductility and workability during the plastic deformation required (Ernst, 2006). During the process of shaping, the material undergoes cold or hot work (Ernst, 2006).

Casting or foundry alloys are designated to be cast right into their final shape (Choundary 2007). The chemical composition of casting alloys, therefore, is usually tailored for good casting properties (Ernst, 2006). Each of these families of alloys can be subdivided into

heat treatable and non heat treatable (International Aluminium Institute, 2008; Choundary 2007). Heat treatment of castings results in improved mechanical properties and temper designations (e.g. O, T4, T6, and T7) are used to identify the heat treatment circle. While as cast alloys are identified by a suffix F following the alloy number (Rashid, 2010).

2.2.2 Aluminium Cast Alloy Designations

Table 2.1: Aluminium Alloy classification system

1xx.x	Unalloyed composition (Al 99.0 or greater)
2xx.x	Copper
3xx.x	Silicon with magnesium and/or copper
4xx.x	Silicon
5xx.x	Magnesium
6xx.x	Magnesium and Silicon
7xx.x	Zinc
8xx.x	Tin
9xx.x	Unused

* 190.x indicates commercially pure aluminium with 99.90% purity

* Digit on the right of decimal point indicates the product form: 0 – castings 1 – ingots

Source: Rashid, 2010

2.3 Al-Si Foundary Alloys

Al-Si alloys can be cast using a variety of techniques: the most commonly used techniques are sand casting, gravity die casting and injection mould casting (Lozano and Voort, 2010). Sand casting is the most versatile technique and permits manufacturing of the largest castings-weights approaching 10,000 kg is possible. Infact, sand casting is best for larger castings and low production runs. The surfaces are the roughest of these methods and dimensional tolerances are the greatest (Rashid, 2010).

Die casting is the highest productivity method of the three. Molten metal is injected into a cavity made from heat treated tool steel under pressures up to 140 Mpa. Castings are often smaller than 5 kg but larger castings up to 50 kg are possible, depending upon the equipment available. Die cast parts have smooth surfaces and require little, if any, machining. Die castings permits production of thinner walls than the other methods (Lozano and Voort, 2010). Permanent mould casting is performed using either gravity or pressure feeding of the liquid metal into a permanent mould. Casting sizes may be somewhat larger than for die casting. Surfaces are also quite smooth. Both die casting and permanent mould casting produce rapid solidification rates that yield fine microstructures and good properties (Lozano and Voort, 2010).

Cast Al-Si alloys usually have casting defects such as porosity and inclusions, which can greatly degrade the mechanical properties of the materials (Bangyikhan, 2005). A pore is a kind of stress concentrator, and thus can lead to micro-crack initiation and propagation. Microporosity usually results from absorption of dissolved gas from the melt and or failure of interdendritic feeding.

Solubility of hydrogen in Al-Si melts increases as temperature increases (Ye, 2003; Bangyikhan, 2005). When molten Al-Si alloy solidifies, the hydrogen atom precipitates from the melt and form molecular hydrogen. If alloy solidifies faster than the molecular hydrogen escapes from the melt, gas porosity will be generated in the solid alloy (Ye, 2003). On the other hand, a lot of dendritic structures form in Al-Si alloys during its solidification and reduce the fluidity of melt (Bangyikhan, 2005). Thus the shrinkage in the melt between the dendrites cannot be fully filled, and microporosity is formed along these dendrites after the melt solidification (Ye, 2003).

Alloying elements greatly influence porosity formation via a few mechanisms. First, an alloying element can change the freezing range of Al-Si alloys so that the porosity can be changed. When the freezing range is decreased, the "mushy zone" in the solidifying material is reduced and thus the porosity is reduced. Second, alloying element can form dendritic intermetallic during solidification. Porosity can form along these intermetallic dendrites (Ye, 2003).

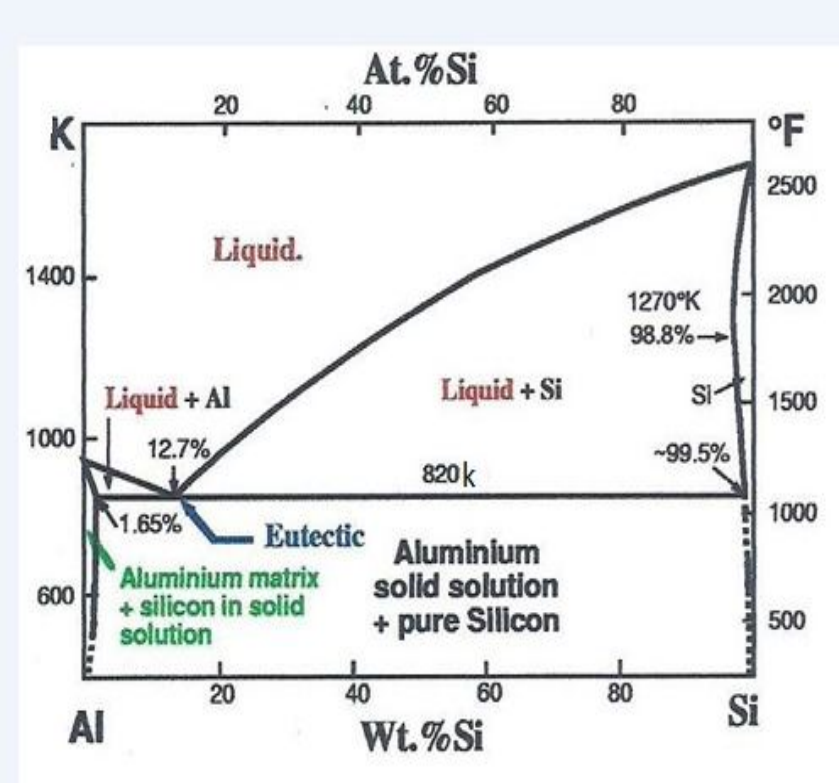


Figure 2.1: Al-Si cast alloy phase diagram (Jacobs, 1999)

The melting points of Al and Si are respectively 660^{o}C and 1414^{o}C, while the eutectic reaction occurs at 12.7 wt% Si. The maximum solubility of Si in Al occurs at the eutectic temperature and is 1.65 wt% (Lozano and Voort, 2010). When the eutectic point is reached, the eutectic Al-Si phase nucleates and grows until the end of solidification. At room temperature, hypoeutectic alloys consist of a soft and ductile primary aluminium phase and a hard and brittle eutectic silicon phase (Ye, 2002; Jacobs, 1999). Hyper eutectic alloys usually contain coarse, angular primary silicon particles as well as a eutectic silicon phase (Ye, 2002). Modifiers like Na shift the eutectic to a higher Silicon content around

14wt%, preventing precipitation of proeutectic Si while refining the structure of the eutectic (Lozano and Voort, 2010).

2.4 Ternary diagram in Al-Si-Mg alloy

Ternary diagrams enable more expedient alloy compositions to be selected and help Metallurgist to understand the various processes that occur in such systems (Choundary, 2007). The description of equilibrium in a two-component system at a fixed pressure is represented by a plane figure, since only two variables are required i.e. Temperature and Composition. For a system at constant pressure in a ternary diagram, three compositions variables (two of them independent) and a temperature variable must be represented. The description of phase equilibra relating composition and temperature to the phases presented necessitates the use of a three-dimensional diagram (Schaffer *et al*, 1999).

Al-Si-Mg is an alloy with ternary phase diagram. In particular, any alloy has a unique liquidus temperature for each composition of the solid. An important difference from the two component cases is that, in systems of three or more components, the temperature does not uniquely define the solidus and liquidus composition, in general. The simplest example is that of a ternary alloy system, compositions in ternary systems are usually represented as points on or in an equilateral triangle ABC. The corners of the triangle correspond to the three pure components, and the edges represent the three binary system. Each point within the triangle corresponds to a definite composition. The ratio of the three components for the P is equal to the ratio of the distances a, b, c of % from the three sides of the triangle.

The sum of these three distances is constant for a given equilateral triangle (Abdulwahab, 2011).

In a three-component system therefore, there must be a line on a liquidus surface that corresponds to any particular temperature; the ties line are mostly used to indicate the equilibrium relationships.

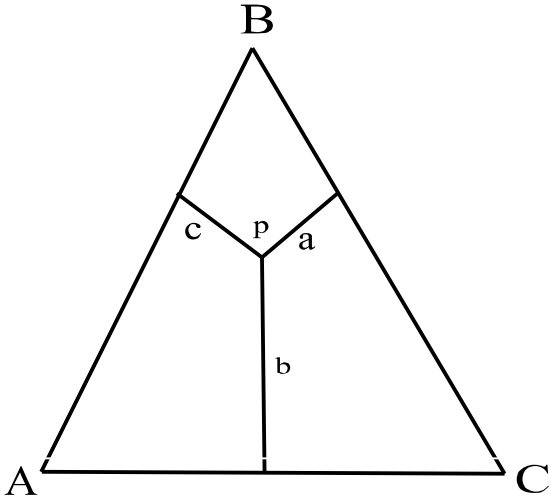


Figure 2.2 Representation of ternary composition (Abdulwahab,

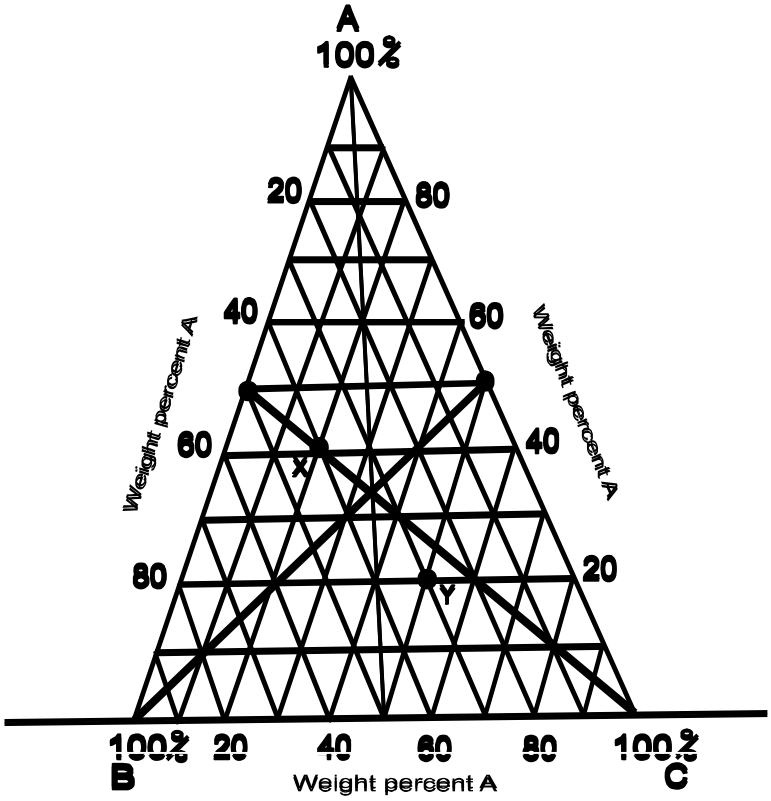


Figure 2.3 Ternary Phase diagram for a composition base for an ABC (Choundary,

The point X is on an iso-composition line AD and thus the % of A in the alloy is 40%. In a seminar manner, draw a line DE and determine that the % of B in the alloy is also 40%. A thick line OF is drawn and the % of C in the alloy is determined to be 20%. Thus the composition of the ternary alloy at point X is 40%A, 40%B and 20%C. Actually only percentages need be determined since the third can be obtained by subtracting the sum of two from 100% (Choundary, 2007)

2.5 Al-Si-Mg alloys

Aluminium cast alloys can be given, by adding a proper amount of Mg, a very strong heat treatment response. Thermal treatment of these Al-Si-Mg alloys allow Mg and Si to dissolve in the aluminium matrix; while upon ageing, Guiner-preston zones or highly dispersed Mg_2Si particles precipitate in the matrix, thereby significantly enhancing the tensile strength (Seifeddine, 2007).

Zhong-Wei *et al*, 2005 reported the effect of Mg on the eutectic Si microstructure and mechanical behaviour of Al-Si-Mg casting alloys. They said that the eutectic Si particles are larger in the alloys with increase in Mg content, and the yield stress increases. The tensile ductility is decreased with increase in Mg content.

2.6 Heat Treatment 0f Cast Al-Si-Mg alloys

Heat treatment is one of the major factors used to enhance the mechanical properties of heat-treatable Al-Si-Mg alloys, through an optimization of both solution and ageing heat treatments given to these alloys. The solution treatment homogenizes the cast structure and

minimizes segregation of alloying elements in the casting. The segregation of solute elements resulting from dendritic solidification may have an adverse effect on mechanical properties (Tash, 2007). Typical heat treatment process for cast Al-Si-Mg alloy is T6-temper condition, which consist of a solution heat treatment, quenching and ageing at an elevated temperature (Ma, 2006). Basically it is a two steps procedure; first a single phase supersaturated solid solution is produced by heating the material at a temperature where the phase diagram exhibits a maximum solubility, generally at a eutectic temperature, followed by rapid quenching at room temperature. This step is then followed by an ageing procedure consisting in maintaining the sample at a room temperature (natural ageing or T4) or a higher temperature generally around 200^{o}C (artificial ageing or T6) where a hardness peak is observed. This process produces precipitates evolving from the so-called Guinier-Preston zones to coarse incoherent precipitates (β) when the equilibrium is reached. The hardness peak is for the most part due to the presence of fine intermediate (coherent/semi-coherent) precipitates (β'/β") which harden the matrix upon a subsequent deformation process (Dirras, 2010).

2.6.1 Effect of Solutionizing Temperature and time on Al-Si-Mg alloy

A solutionizing treatment of cast Al-Si-Mg alloys in the range of 400-560^{o}C dissolves the hardening agents (Mg_2Si particles) into the α-Al matrix, reduces the micro-segregation of magnesium, cupper, manganese, and other addition elements in aluminium dendrites, and spheroidizes the eutectic Silicon particles to improve the ductility (Fracasso, 2010; Ma, 2006). The amount and rate of dissolution increase with increasing solution treatment temperature, but the temperature is limited by the solid temperature (Ma, 2006). The

desired solutionizing treatment time and temperature to a great extent depend on the casting method, the extent of modification and desired level of spheroidization and coarsening of Silicon particles (Ma, 2006).

Fracasso, 2010 discovered that the required time has to be enough to arrive at an entirely homogenous structure, the time depends on several parameters, as chemical composition, temperature, structure coarseness, casting method and phases to dissolve.

2.6.2 Effect of quenching rate

The objectives of quenching are to suppress the precipitation and to retain solute atoms and quenched-in vacancies in solution (Ma, 2006). The quenching help to preserve the structure existing at high temperature. The main intension is to avoid formation of precipitates or second phases during cooling (Fracasso, 2010).

According to Fracasso, 2010, the phases require different time to start their formation. If the cooling rate is fast enough to avoid the formation of second phases, the final structure will be a unique solution made of uniformly distributed solute atoms inside the matrix.

The quenchants used for aluminium alloys include water, brine solution and polymer solution (Bangyikhan, 2005). Water quenching is mostly used for aluminium alloys, but it causes distortion, cracking and residual stresses (Ma, 2006). This problem can be tackled in two ways; one method is increasing the water temperature so that the temperature gradient between water and the part being quenched can be reduced. The other method use

the polymer solution as a quenchant which is widely employed since the distortion problem can be effectively reduced by varying the polymer concentration (Ma, 2006).

2.6.3 Effect of ageing time and temperature

During the early ageing stages of an Al-Si-Mg alloy, the saturated solid solution first develops solute clusters. However, the supersaturation of vacancies allows diffusion, thus leading to the formation of GP zones. A state of under ageing can be maintained. This state is known to be associated with a microstructure consisting primarily of needle-shaped or spherical GP zones, needle-like β'' (Mg_2Si) and rod-like β^1 (Mg_2Si) transitional phases (Tash, 2007).

According to Tash 2007, the hardness increases with ageing temperature up to 180^oC (peak temperature) for 356 alloys in the unmodified and modified conditions, followed by a decrease in hardness at 200 and 220^oC (over ageing). The coherent rods or needles of β^1 (Mg_2Si) and incoherent equilibrium β phase dominate the microstructure.

After the common thermal treatments, these alloys contain three phases; (i) the Al matrix, (ii) Si (large particles, coarse dispersion), and Mg_2Si (small particles, fine dispersion). The precipitation sequence of alloy with an atomic ratio Mg:Si of 2:1 is Supersaturated α – G.p zones – β^1 – β (Mg2Si) (Ernst, 2006)

G.P zones – is an abbreviation for Guiner-preston zones; an early stage of precipitates characterized by an enrichment of solute atoms (Si, Mg) on the lattice sites of the matrix

(Al). In the case of Al-7% Si-0.3% Mg alloys, these first particles have the shape of needles, oriented along <100> directions of the Al-matrix (Ernst, 2006).

The particle that form in the next stage of the decomposition process, β^1 particles, already have the composition Mg_2Si. The crystal structure is face centred cubic. The particles are rod-shaped, with the long axis parallel to the <100> directions of the Al-matrix (Ringer and Hono, 2000). The equilibrium phase, β (Mg_2Si), finally, has a face centred cubic crystal structure. It is generally believed that the transformation β^1–β is diffusionless with only minor atomic-re-arrangement and some change in the degree of coherency between the precipitate and the matrix (Ernst, 2006).

2.7 Hardness Measurement of Al-Si-Mg alloy

Hardness is a measurement of the resistance of a metal to a permanent plastic deformation (Kokani, 2004). The hardness of Al-Si-Mg alloy is measured by compressing an indenter on its surface. The indenter, that is usually a sphere, pyramid or a cone, is constituted by a material harder than the material on test. The materials commonly used for indenters, for example, are tempered steel, tungsten carbide or diamond. There are three different methods for the hardness measurement: Brinell, Vickers and Rockwell (Avner, 1997). With each tests, the resultant hardness value is determined, in order to have an estimation of the characteristics of resistance of a material to plastic deformation and to have a method of control of quality, particularly to verify the efficiency of the hardening treatment of the materials (Fracasso, 2010).

2.7.1 Rockwell hardness test

The test consists of penetrating into a piece at two times and with two different loads (initial and total), a unified indenter (diamond cone or tempered steel sphere) and to measure the increase of depth between the initial imprint and the final in the suitable time (Fracasso, 2010). Four sizes of hard ball from $^{1}/_{16}\,in$ to $^{1}/_{12}\,in$ ball and the diamond penetrator are most commonly used. The penetrator chuck is mechanically connected to a dial indicator which responds to vertical motion of the penetrator. Since the penetrators are small, the specimen should be ground smooth and clean (Avner, 1997).The specimen is placed on the anvil of the machine and the penetrator seated by means of 10 kg minor load. The dial indicator is zeroed and then a major load of 60,100 or 150 kg is applied, forcing the penetrator into the specimen. Upon removal of major load, the indented specimen recovers slightly, and the final depth of penetration is registered directly on the dial indicator as a hardness number (Avner, 1997).The two commonest scales are the HRB scales and the HRC scales respectively, standing for the 1/16" ball with 100 kg load, and the diamond penetrator with the 150 kg major load. In general, very hard materials are tested with the diamond penetrator.

2.8 Microstructure of Al-Si-Mg alloy

Microstructure of Al-Si-Mg alloys depends strongly both on composition and the casting process. The rapid cooling in pressure die casting causes fine eutectic structure, small primary aluminium dendritic cells and arm spacing, and reduced grain size. Slower rates encountered in permanent mould and sand casting necessitates the use of modifiers such as

strontium or sodium to obtain a finely dispersed eutectic silicon phase (Rashid, 2010). The microstructure of Al-Si-Mg alloys in the as-cast state consist of primary grains of α-Al solid solution with interdendritic regions of Al-Si eutectic, in which various intermetallic phases are present (Kliauga *et al*, 2008). Modification alters the morphology of the eutectic silicon, by changing it from acicular or lamellar to fibrous with the addition of strontium or sodium (Ernst, 2006). The microstructure and alloy constituents are necessitated to achieve optimum mechanical properties (Zhang *et al*, 2005).

2.9 Mechanical Properties of Al-Si-Mg alloy

In solidification process of Al-Si-Mg alloy, grain refinement is very important. Equiaxed grain structures ensures uniform mechanical properties, reduced ingot cracking, improved feeding to eliminate shrinkage porosity, distribution of second phases and microporosity on a fine scale as well as improved machinability of castings (Zhang, 2005). Dendrite cell size, which is controlled by solidification rate, is another important indicator of the mechanical properties of aluminium casting alloys, the ultimate tensile strength and elongation are enhanced by the reduction in cell spacing (Jaber *et al*, 2000). It is well known fact that mechanical properties of Al-Si-Mg alloys are strongly related to the size, shape and distribution of eutectic silicon present in the microstructure. The eutectic silicon morphology, dendrite arm spacing (DAS), grain size all play a vital role when the alloy is put into specific use (Kumar *et al*, 2007). In order to improve mechanical properties, the alloy is generally subjected to modification melt treatment, which transforms the acicular silicon morphology to fibrous one resulting in a noticeable improvement in elongation and strength (Zhang *et al*, 2005; Kumar *et al*, 2007; Tash *et al*, 2007).

2.10 Pre-ageing/interrupted ageing treatment in Al-Si-Mg alloy

Interrupted ageing treatment is a heat treatment that involves interrupting a T6 treatment by ageing at a lower temperature (< 180^{o}C) for an extended period of time before the T6 treatment is resumed until peak hardness is obtained (Risanti *et al*, 2009).It is reported that for most Al alloys, this treatment could display simultaneous improvements in strength and fracture toughness (Hong *et al*, 2006).

2.11 Corrosion Properties of aluminium alloys

Aluminium and its alloys are considered to be highly corrosion resistant under the majority of available service condition. The various grades of pure aluminium are most resistance, followed closely by the Al-Mg, Al-Mn alloys. Next in order is Al-Mg-Si and then Al-Si alloy (Abdulwahab *et al*, 2011). Since commercial purity aluminium alloys contain numerous constituent particles that have electrochemical potentials different from that of the matrix, corrosion pits can readily develop at these particles. Once corrosion pits are formed, they act as stress concentration sites leading to stress corrosion cracking (Reda *et al*, 2008).Metallurgical factors that can affect corrosion in an alloy include; crystallography, grain size and shape, grain heterogeneity, impurity inclusions, and residual stress due to cold work (Rawajfeh and Qawabah, 2009).The corrosion resistance of Al alloy can be modified by heat treatment (Feng *et al*, 2008). It is known that Al alloys with T6 treatment possess high strength, their localized corrosion resistance is poor (Reda *et al*, 2008; Feng *et al*, 2008). To increase this corrosion resistance, over-ageing treatments have been developed (Reda *et al*, 2008). However, the strength of Al alloys with this over-

ageing treatment is decreased (Rawajfeh and Qawabah, 2009; Feng *et al*, 2008). The Al alloy with retrogation and re-ageing treatment posses' high strength and good SCC resistance (Feng *et al*, 2008). However, the RRA treatment cannot be used for large section Al alloy due to its very short retrogression time. To keep strength high and maintain corrosion resistance, novel heat treatment has been developed called high temperature pre-precipitation (HTPP) ageing treatment (Feng *et al*, 2008).

2.12 Corrosion Monitoring and Measurement

There are wide ranges of corrosion monitoring and measurement techniques as follows (Kakani, 2004):

2.12.1 Direct Method

This method consists of visual/optical measurement and weight loss of coupon.

2.12.1.1 Visual/Optical Measurement

This method requires the corroded material to be subjected to visual inspection and physical measurement. This is only possible in those areas where access is available and when plant is shut-down.

2.12.1.2 Weight loss of coupon

This method is used in industry. First, the coupons are measured carefully and their physical dimensions are also recorded. The exposed area of coupons to corrosive

environment is also recorded. One can obtain the rate of corrosion by putting the coupons under actual operating conditions. One will have to inspect these samples at regular intervals and record the results. The loss of weight, after removal of corrosion products is determined and expressed in mil/year. However, this process is a long and tedious, but gives quite reliable results than many of the laboratory tests.

2.12.2 Linear polarization resistance (LPR)

LPR is a widely used electrochemical technique and can be used 'on line' to provide an instantaneous or continuous measurement of the corrosivity of the process stream (Kakani, 2004). This is widely used in the oil field particularly in water systems. In order to determine the corrosion current density and hence corrosion rate, a small potential or current perturbation is applied. To a close approximation, for a corroding electrode, the applied potential and current density are linearly related. One can relate their ratio 'LPR' or polarisation resistance (*Rp*) to the corrosion current density through the following relation (Kakani, 2004):

$$\text{Icorr} = \frac{\text{constant}}{\text{Rp}}$$

We may note that the above relation only holds if the electrode is polarised well from the corrosion potential

2.12.3 Electrical Resistance (ER) Equipment

This operates on the basic principle that electrical resistance increases as the cross-sectional area of a metallic conductor decreases. The probe is the heart of an ER

equipment, which is introduced in the corrosive environment and with which corrosion measurements are made. The probe acts as an in-situ sensor that accumulates the corrosion history of the environment and displays or records the corrosion information on an instrument. The basic function of an ER instrument is to compare the resistance of an element that is exposed to corrosion with the resistance of an element that is protected from corrosion. If the resistance of an exposed element is measured directly, the data will be affected by element thickness and temperature. With this

method, temperature changes, that equally affect both elements, are cancelled out and the data obtained are inversely proportional to the thickness of the exposed element. This is why, the ER probe is often referred to as an electrical coupon. We may note that there is an important difference between ER and coupon system, i.e., the coupon has to be removed from the pipe to measure the corrosion rate whereas the probe remains in the system at all times. To know the corrosion rate, electrical resistance changes are converted into thickness changes which can be plotted against time to know the corrosion rate (Kakani, 2004).

2.13 Mechanism of electrochemical corrosion

Electrochemical corrosion involves two half cell reactions; an oxidation reaction at the anode and a reduction reaction at the cathode (Abdulwahab 2011, Perez, 2004). For corrosion of Aluminium in water with a near neutral pH, these cell reactions can be represented as;-

Anode reaction $Al=Al^{3+} + 3e^{-}$ 2.3

Cathode reaction $0_2 + 2H_2O + 4e^- = 4(OH)^-$ …….....2.4

Overall reaction $4Al+30_2+6H_2O = 4Al^{3+} + 12(OH)^-$ ……2.5

There are obviously different cathodic reactions for different alloys exposed to various environments. These half cell reactions are thought to occur (at least initially) at microscopic anodes and cathodes covering a corroding surface. Microscopic anodes and cathodes can develop as corrosion damage progress with time (Abdulwahab, 2011, Perez, 2004; Abdulwahab *et al*, 2011; Abdulwahab, 2007).

In seawater environment, the cell reactions are;

Cathode reaction $NaCl = Na^+ + Cl^-$……2.6

Overall reaction $2Al + 6Cl^- = 2Al^{3+} + 3Cl_2$……...2.7

2.14 Forms of corrosion

It is convenient to classify corrosion according to the manner in which it manifests.

2.14.1 Uniform Attack

Uniform attack is a form of electrochemical corrosion that occurs with equivalent intensity over the entire exposed surface and often leaves behind a scale or deposit. In a microscopic sense, the oxidation and reduction reactions occur randomly over the surface. Some familiar examples include general rusting of steel and iron and the tarnishing of silverware.

This is probably the most common form of corrosion. It is also the least objectionable because it can be predicted and designed for with relative ease (Callister, 2001).

2.14.2 Pitting

Pitting is another form of localized corrosion attack in which small pits or holes form (Perez, 2004). They ordinarily penetrate from the top of a horizontal surface downward in a nearly vertical direction. It is an extremely insidious type of corrosion, often going undetected and with very little material loss until failure occurs. The mechanism for pitting is probably the same as for crevice corrosion in that oxidation occurs within the pit itself, with complementary reduction at the surface. It is supposed that gravity causes the pits to grow downward, the solution at the pit tip becoming more concentrated and dense as pit growth progresses. A pit may be initiated by a localized surface defect such as a scratch or a slight variation in composition. In fact, it has been observed that specimens having polished surfaces display a greater resistance to pitting corrosion (Callister, 2001).

2.14.3 Intergranular Corrosion

Intergranular corrosion occurs preferentially along grain boundaries for some alloys and in specific environments. The net result is that a macroscopic specimen disintegrates along its grain boundaries. This type of corrosion is especially prevalent in some stainless steels. When heated to temperatures between 500 and 800^{o}C for sufficiently long time periods, these alloys become sensitized to intergranular attack (Callister, 2001). It is believed that this heat treatment permits the formation of small precipitate particles of chromium carbide ($Cr_{23}C_6$) by reaction between the chromium and carbon in the stainless steel. Both the

chromium and the carbon must diffuse to the grain boundaries to form the precipitates, which leaves a chromium-depleted zone adjacent to the grain boundary. Consequently, this grain boundary region is now highly susceptible to corrosion. Intergranular corrosion is an especially severe problem in the welding of stainless steels, when it is often termed weld decay (Callister, 2001).

2.14.4 Stress Corrosion

Stress corrosion, sometimes termed stress corrosion cracking, results from the combined action of an applied tensile stress and a corrosive environment; both influences are necessary (Perez, 2004). In fact, some materials that are virtually inert in a particular corrosive medium become susceptible to this form of corrosion when a stress is applied. Small cracks form and then propagate in a direction perpendicular to the stress, with the result that failure may eventually occur. Failure behavior is characteristic of that for a brittle material, even though the metal alloy is intrinsically ductile. Furthermore, cracks may form at relatively low stress levels, significantly below the tensile strength. Most alloys are susceptible to stress corrosion in specific environments, especially at moderate stress levels. For example, most stainless steels stress corrode in solutions containing chloride ions, whereas brasses are especially vulnerable when exposed to ammonia.

The stress that produces stress corrosion cracking need not be externally applied; it may be a residual one that results from rapid temperature changes and uneven contraction, or for two-phase alloys in which each phase has a different coefficient of expansion. Also, gaseous and solid corrosion products that are entrapped internally can give rise to internal stresses (Callister, 2001).

2.14.5 Hydrogen Embrittlement

Various metal alloys, specifically some steels, experience a significant reduction in ductility and tensile strength when atomic hydrogen (H) penetrates into the material. This phenomenon is aptly referred to as hydrogen embrittlement (Kakani, 2004). The terms hydrogen induced cracking and hydrogen stress cracking are sometimes also used. Strictly speaking, hydrogen embrittlement is a type of failure; in response to applied or residual tensile stresses, brittle fracture occurs catastrophically as cracks grow and rapidly propagate. Hydrogen in its atomic form (H as opposed to the molecular form, H_2) diffuses interstitially through the crystal lattice, and concentrations as low as several parts per million can lead to cracking (Callister, 2001). Furthermore, hydrogen induced cracks are most often transgranular, although intergranular fracture is observed for some alloy systems. A number of mechanisms have been proposed to explain hydrogen embrittlement, most of them are based on the interference of dislocation motion by the dissolved hydrogen. Hydrogen embrittlement is similar to stress corrosion in that a normally ductile metal experiences brittle fracture when exposed to both a tensile stress and a corrosive atmosphere (Callister, 2001).

Table 2.2: Methods for Corrosion Measurement

S/N	Methods	Techniques
1	Non –Destructive testing (NDT)	Intelligence testing, ultrasonic testing, radiography testing, thermography, eddy current, magnetic flux
2	Analytical method	pH measurement, dissolved gases (CO_2, H_2, O_2)
3	Fluid electrochemistry	Ac impedence, potential, potentiostatic, potentiodynamic measurement
4	Operational data	Pits, pressure, temperature, velocity or flow rate
5	Corrosion monitoring	Weight loss coupons, hydrogen penetration, galvanic current, electrical resistance, linear polarization

Source: (Abdulwahab, 2011)

2.15 Applications of Aluminium and its alloys

Aluminium and aluminium alloys are extensively used for commercial applications due to its desirable properties, such as, low density, high thermal conductivity, good corrosion resistance, high castability, high machinability and formability, low cost (International Aluminium Institute, 2008; Haghshenas *et al*, 2008; Leo and Cerri, 2003; ASM, 1978).

The wide range of application of aluminium and its alloys include;-

1 Its application for the manufacture of domestic cooking utensils, such as kettles, cooking pots, frying pans, spoons and plates. This is possible due to its high thermal conductivity and good corrosion resistance.

2 Used as electrical conductors, for example, in electricity transmission lines.

3 Used extensively in the agricultural industry, particularly in food industries, as containers for food packaging.

4 In the alloy form, it is mostly used for mechanical applications such as for the manufacture of engine blocks for cars and motor cycles, and manufacture of car bodies.

5 Extensively used for building construction example, as roofing, casement windows and in the form of paint to protect other metals like steel from atmospheric deterioration (Umaru, 2009).

Basically, A356 alloy find application in automobile and marine. In the auto-industry, the alloy is used as brake callipers, carburettor parts, etc. While in marine they are useful as drill pipes.

CHAPTER THREE

MATERIALS AND METHOD

3.1 Materials and equipment

Some of the materials and equipment used in this research are listed below

3.1.1 Materials

The materials used in this research include; high purity aluminium wire (Al), pure silicon powder (Si), Magnesium (Mg), iron (Fe), Copper (Cu), Zinc (Zn), Titanium foil (Ti), Ferromanganese and elemental sodium (Na). Others are bentonite, moulding boxes and crucible sourced from the Department of Metallurgical and Materials Engineering, Ahmadu Bello University, Zaria.

3.1.2 Equipment

The following equipment were used; Muffle electrical resistance furnace (used for the heat treatment with capacity of 1200^{o}C), Labotech water heater (comprised of heating coil, used to heat up the water for quenching), Rockwell hardness tester (Indentee universal hardness tester 8187.5KLV) used for the hardness determination, Digital weighing balance, Polishing machine, Optical microscope, SEM machine (it output are basically either back scattered electrical image or secondary electron image. It can be equipped with EDS).

3.2 Methods

3.2.1 Casting of the samples

The Al-Si-Mg alloy with charge calculation values as presented in Table 3.1 was produced in this work. Using the method described in Abdulwahab 2007, the high purity aluminium wire was melted using a muffle resistance furnace that was allowed to heat to 750^{o}C. The crucible was then removed from the furnace, and the alloying elements added before returning to the furnace for further 30 minutes, during which the furnace temperature was raised to 800^{o}C for superheat to occur. Elemental sodium (0.01% Na) was then added and stirred thoroughly before pouring into the mould. The cast samples which were machined to hardness and corrosion samples dimension (i.e. 20mm by 10mm) were used.

Table 3.1: Charge calculation of the Al-Si-Mg alloy produced (wt %).

Al	Si	Mg	Fe	Cu	Mn	Zn	Ti	Na
92.14	7.0	0.3	0.08	0.03	0.03	0.03	0.03	0.01

3.2.2 Heat treatment of the Al-Si-Mg alloy

A total of three hundred and thirty six samples for hardness, corrosion, SEM and OPM were solution heat treated at a temperature of 540^{o}C for 1h in an electrical heat treatment furnace and then rapidly quenched in warm water (65^{o}C). The quenched samples were given double-thermal ageing; by varying the pre-ageing temperatures and time, DTA and single thermal ageing, STA treatments as described below.

3.2.2.1 Double Thermal Ageing Treatment (DTAT)

Three hundred and fifteen Samples were given a double-thermal ageing treatment consisting of pre-ageing at temperatures of 90^{o}C, 105^{o}C and 120^{o}C for 1-5 h each, and then finally aged at180^{o}C for 2 h i.e.

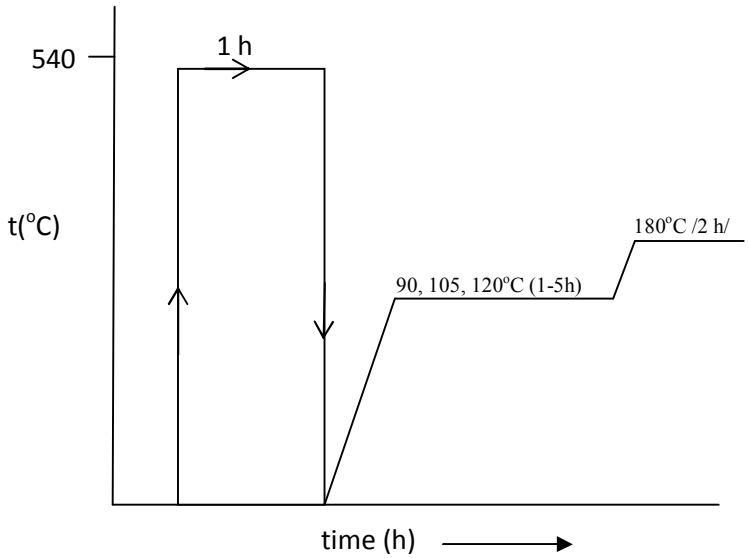


Fig 3.1: Schematic diagram of the DTAT heat treatment cycle indicating pre-ageing regions

The conventional heat treatment was performed on twenty one samples, by heating to 540^{o}C for 1h, after which the samples were quenched in warm water. The samples were further aged to 180^{o}C for 2 h.

3.2.3 Hardness measurement

The hardness characteristic of 17 samples (15 for DTAT, 1 for STAT and 1 for as-cast) was measured using a Rockwell hardness tester with a minor load of 10 kgf and a total load of 60 kgf. The (scale F: HRF) was used in order to obtain a reliable average hardness

reemploying 1/16 diameter ball indenter with 100 kg load in accordance with the report elsewhere (Aye *et al*, 2008).

3.2.4 Electrochemical Corrosion Technique

The electrochemical corrosion techniques used in this research are: weight loss and linear polarisation corrosion study.

3.2.4.1 Weight loss

A total of 340 coupons were used for the test; 300 each for DTAT, 20 each for STAT, and 20 each for as-cast samples respectively. Before immersion, the coupons were cleansed, weighed and stored in the desiccator. Sets of same concentration of simulated seawater were made, by providing a solution containing 3.5g of NaCl in 100mL of distilled water. The cleaned coupons were suspended into the simulated seawater with the aid of threads. The weight losses of the coupons were taken at interval of two days over a period of forty (40) days. After removal from the solution, each coupon was weighed. The surface was scrubbed with brush in distilled water, rinsed in ethanol and then air-dried.

3.2.4.1.1 Corrosion Rate Determination

The weight loss method of estimating the corrosion rate was employed. The weight loss was determined by finding the difference between the initial weights of the coupons and the final weights after two days interval using the following relationship.

$$W = W_0 - W_f \quad \text{.....3.1}$$

The corrosion rate was determined in mm per year (mm/yr) using the relationship (Abdulwahab, 2007).

$$\text{Corrosion rate (mm/yr)} = \frac{87.6W}{DAT} \quad \text{.....3.2}$$

Where;-

W= weight loss (mg)

D= density of the materials, g/cm^3

A = exposed surface area (cm^2)

T = total time of immersion (hr)

W_0 = initial weight of coupons

W_f = final weight of coupons

3.2.4.2 Linear Polarisation corrosion study

The electrochemical potentiodynamic technique was used to characterize the corrosion rate (current densities) of some samples which consist of cyclic polarization scan employing the linear polarization technique according to ASTM G 3-89 and ASTM 5-94 standards. A potentiostat coupled to a computer system, a glass corrosion cell kit with graphite rods as the counter electrodes and a saturated Ag/AgCl 3M KCl electrode as the reference electrode (SCE) were used. The conventional three electrode electrochemical cell system was used. The electrochemical cell was made of 500 ml Pyrex glass conical flask suitable

for the conventional three-electrode system. The cover of the cell had five holes for the reference electrode, working electrode, counter electrode, temperature measurement and aeration/de-aeration. The working electrodes consist of the thermally treated samples. The samples were positioned at the glass corrosion cell kit, leaving a 3.808 cm^2 alloy surfaces in contact with the solution. Polarization test were carried out in a 3.5wt% NaCl solution (3.5 g in 100 mL of distilled water) at room temperature (RT) in a static solution for a period of 30 minutes each using a potentiostat. The polarization curves were determined by stepping the potential at a scan rate of 0.003V/sec. The polarization curves were plotted using Autolab data acquisition system. Electrochemical measurements were carried out with the General Purpose Electrochemical Software (NOVA 3.0) package. The corrosion rate and potential were estimated by the Tafel extrapolation method (corrosion rate analysis) using both the anodic and cathodic branches of the polarization curves. All the measurements were made at room temperature using 3.5 % NaCl solution. The polarisation corrosion study was done in centre for scientific and industrial research, nano structured centre, Pretoria- South Africa.

3.2.4.3 Linear Polarisation corrosion Measurement

When a metal/alloy electrode is immersed in an electrolytically conducting liquid of sufficient oxidizing power, it will corrode by an electrochemical mechanism. This process involves two simultaneous complementary reactions. At anodic sites, metal will pass from the solid surface into the adjascent solution and, in so doing, leave a surplus of electrons at the metal surface. The excess electrons will flow to nearby sites, designated cathodic sites,

at which they will be consumed by oxidizing species from the corrosive liquid (Auwal, 2012).

The corrosion current (I_{CORR}), generated by the flow of electrons from anodic to cathodic sites, could be used to compute the corrosion rate by the application of a modified version of Faraday's Law.

$$C = \frac{I_{CORR} \times E}{A \times D} \times 128.67 \quad \text{.....} \quad 3.1$$

Where:

C = Corrosion rate in "mils per year" (mpy)

E = Equivalent weight of the corroding metal (g)

A = Area of corroding electrode (cm^2)

D = Density of corroding metal (g/cm^3)

However, anodic and cathodic sites continually shift position, and they exist within a continuously conductive surface, making direct measurement of I_{CORR} impossible. Small, externally-imposed, potential shifts (ΔE) will produce measurable current flow (ΔI) at the corroding electrode. The behaviour of the externally imposed current is governed, as is that of $I_{CORR,}$ by the degree of difficulty with which the anodic and cathodic corrosion processes takes place. The greater the difficulty, the smaller the value of I_{CORR} , and the smaller the value of ΔI for a given potential shift. In fact, at small values of ΔE, ΔI is directly

proportional to I_{CORR}, and hence to the corrosion rate. This relationship is embodied in the theoretically derived Stern-Geary equation:

$$\Delta E/\Delta I = \frac{ba\ bc}{2.3\ i_{CORR}\ (ba+bc)} \quad \text{.....} \quad 3.2$$

The numbers ba and bc are empirical constants, the Tafel constants, so the relationship can be further expressed as

$I_{CORR} = \Delta I/\Delta E \times$constant.

The value $\Delta I/\Delta E$ is known as the Polarisation Resistance (Auwal, 2012)

3.2.5 Microstructural examination

Metallographic specimens were cut from the DTAT, STAT and as-cast alloys. The cut specimens were then mounted in Bakelite and mechanically ground progressively on grades of SiC impregnated emery paper (80-600 grits) size using water as the coolant. The ground specimens were then polished using one-micron size alumina polishing powder suspended in distilled water. Final polish was done using 0.5-micron alumina polishing powder suspended in distilled water. Following the polishing operation, etching of the polished specimen was done using Kellers reagent and the micrographs obtained were then recorded using an optical microscope with built in camera and a Field Emission scanning electron microscope equipped with energy dispersive spectrometer (FE-SEM/EDS) with model: Joel JSM-7600F.

CHAPTER FOUR

RESULTS AND DISCUSSION

4.1 RESULTS

The hardness of Al-Si-Mg alloy in the as-cast, unmodified and modified in various heat treated condition are shown in Tables 4.1 - 4.5. Table 4.6 shows data on corrosion rate of treated samples and as-cast, while Table 4.7 shows hardness of some samples after corrosion in simulated sea water environment. Tables 4.8 - 4.10 show values of the kinetic corrosion parameters at different temper conditions. Figures 4.1 - 4.4 represent the hardness variation with thermal treatment of samples, while Figures 4.5 - 4.8 represent the correlation of corrosion characteristics with thermal treatment. The FE-SEM/EDS microstructures of some treated alloys can be found in Plates 1 - 4. The OPM of the as-cast and solution heat treated (SHT) samples is presented in Plates 5a and 5b, while that of some as-corroded samples are presented in Plates 6 a-d.

Tables 4.1: Hardness value of Al-Si-Mg alloy after DTAT at 90^{o}C

Ageing time (h)	HRF
1	4.8
2	5.1
3	6.7
4	5.0
5	4.2

Tables 4.2: Hardness value of Al-Si-Mg alloy after DTAT at 105^{o}C

Ageing time (h)	HRF
1	6.4
2	5.1
3	6.2
4	7.4
5	7.2

Tables 4.3: Hardness value of Al-Si-Mg alloy after DTAT at 120^{o}C

Ageing time (h)	HRF
1	7.0
2	4.7
3	18.2
4	9.8
5	4.0

Tables 4.4: Comparison of peak ageing time for DTAT at different ageing temperatures and STAT Al-Si-Mg alloy

Ageing temperature (^{o}C)	Peak ageing time (h), t_p
90	3
105	4
120	3
STAT 180-2h	2

Tables 4.5: Comparison of peak hardness for DTAT at different ageing temperatures, STAT and as-cast Al-Si-Mg alloy

Ageing temperature(^{o}C)	Peak hardness (HRF), Hp
90	6.7
105	7.4
120	18.2
STAT 180-2h	4.2
As-cast	3.8

Table 4.6: Comparative study of corrosion rate from weight loss in simulated sea water after 40days for DTAT-T7, STAT-T6 and as-cast Al-Si-Mg alloy

Ageing condition (^{o}C)/Time (h)	Corrosion rate (mm/yr)
As-cast	0.11298
STAT 180-2 h	0.10491
DTAT 90- 1 h	0.07532
DTAT 90- 2 h	0.06994
DTAT 90- 3 h	0.05918
DTAT 90- 4 h	0.05380
DTAT 90- 5 h	0.04035
DTAT 105- 1 h	0.08608
DTAT 105- 2 h	0.06725
DTAT 105- 3 h	0.05918
DTAT 105- 4 h	0.05380
DTAT 105- 5 h	0.05111
DTAT 120- 1 h	0.09684
DTAT 120- 2 h	0.06725
DTAT 120- 3 h	0.05111
DTAT 120- 4 h	0.04842
DTAT 120- 5 h	0.04842

Table 4.7: Hardness values of some selected Al-Si-Mg alloys after exposure to weight loss corrosion study

Description	Hardness (HRF)
DTAT90-3 h	5.3
DTAT105-4 h	6.3
DTAT120-3 h	17.4
STAT180-2 h	4.1
As-cast	3.6

Table 4.8: Comparative study on Linear Polarisation Corrosion data obtained for as-cast, STAT and DTAT Al-Si-Mg alloy in simulated seawater environment after pre-ageing at 90^{o}C

Samples	ba (V/dec)	bc (V/dec)	Ecorr, Calc (V)	Ecorr, Obs (V)	jcorr (A/cm²)	icorr (A)	Corrosion rate (mm/year)	Polarization resistance (Ω)	E Begin (V)	E End (V)
As-received	0.062881	0.14153	-1.0616	-1.0387	7.58E-06	1.52E-05	0.073489	1247.2	-1.0971	-0.94818
180/2 h	0.13504	0.3217	-1.2676	-1.2128	6.24E-06	1.25E-05	0.060469	3311.3	-1.2436	-1.0776
90/1 h	0.063822	0.22206	-1.2487	-1.2193	1.17E-06	4.45E-06	0.011057	4837.6	-1.2704	-1.0922
90/2 h	0.05879	0.20422	-1.2339	-1.2064	1.15E-06	2.30E-06	0.011126	8637.3	-1.2631	-1.0776
90/5 h	0.12128	0.14212	-1.1283	-1.1394	2.33E-06	4.66E-06	0.022595	6096.7	-1.2436	-1.058

Table 4.9: Comparative study on Linear Polarisation Corrosion data obtained for as-cast, STAT and DTAT Al-Si-Mg alloy in simulated seawater environment after pre-ageing at 105^{o}C

Samples	ba (V/dec)	bc (V/dec)	Ecorr, Calc (V)	Ecorr, Obs (V)	jcorr (A/cm²)	icorr (A)	Corrosion rate (mm/year)	Polarization resistance (Ω)	E Begin (V)	E End (V) (V)
Asreceived	0.062881	0.14153	-1.0616	-1.0387	7.58E-06	1.52E-05	0.073489	1247.2	-1.0971	-0.94818
180/2h	0.13504	0.3217	-1.2676	-1.2128	6.24E-06	1.25E-05	0.060469	3311.3	-1.2436	-1.0776
105/1h	0.037355	0.18736	-1.2309	-1.2091	1.72E-06	3.44E-06	0.016695	3927.3	-1.2534	-1.1093
105/2h	0.15317	0.047975	-1.1587	-1.1394	1.75E-06	3.50E-06	0.016964	4533.4	-1.1826	-1.0361
105/3h	0.13222	0.059814	-1.154	-1.1394	1.61E-06	3.21E-06	0.015575	5566.3	-1.1996	-1.0556

Table 4.10: Comparative study on Linear Polarisation Corrosion data obtained for as-cast, STAT and DTAT Al-Si-Mg alloy in simulated seawater environment after pre-ageing at 120^{o}C

Samples	Ba (V/dec)	bc (V/dec)	Ecorr, Calc (V)	Ecorr, Obs (V)	jcorr (A/cm²)	icorr (A)	Corrosion rate (mm/year)	Polarization resistance (Ω)	E Begin (V)	E End (V)
As-received	0.062881	0.14153	-1.0616	-1.0387	7.58E-06	1.52E-05	0.073489	1247.2	-1.0971	-0.94818
180/2h	0.13504	0.3217	-1.2676	-1.2128	6.24E-06	1.25E-05	0.060469	3311.3	-1.2436	-1.0776
120/1h	0.074668	0.25195	-1.2006	-1.1676	3.86E-07	1.47E-06	0.003647	17041	-1.2167	-1.0361
120/3h	0.17888	0.050518	-1.1872	-1.1676	2.86E-07	1.09E-06	0.002706	15705	-1.1996	-1.0556
120/5h	0.060875	0.23044	-1.1212	-1.0887	3.84E-07	1.46E-06	0.003633	14303	-1.1264	-0.94818

4.2 Discussion

In this study, the first set of experiments was designed to characterize the effect of a pre-ageing temperature and time on the hardness of as-cast, STAT and DTAT Al-Si-Mg alloy. The results are shown in Tables 4.1 - 4.6.

4.2.1 Hardness Measurement and Thermal Ageing Treatments

The Hardness measurement of DTA and STA treatment samples was done with a Rockwell hardness tester (indentee universal) with the HRF scale and discussed below

4.2.1.1As-cast and Single-Thermal Ageing (STAT) Al-Si-Mg alloy

From the Hardness results obtained (Table 4.4), the hardness value of STAT and as-cast were 4.2 HRF and 3.8 HRF respectively. It is obvious from the results shown in Figure 4.1 that as-cast Al-Si-Mg alloy has the lowest hardness value. This infers that modification treatment have an appreciable influence on precipitation strengthening of this alloy.

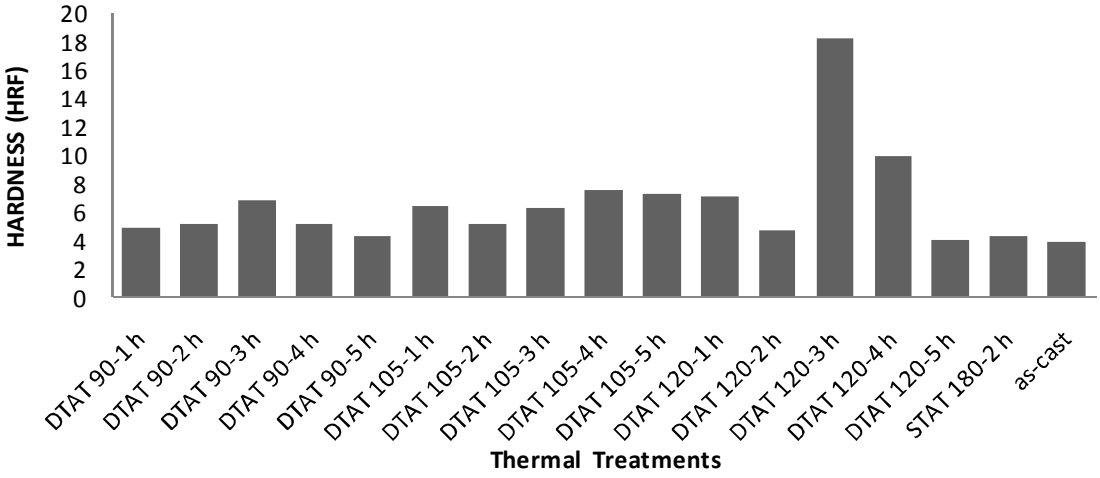


Figure 4.1: Hardness of Al-Si-Mg alloy under different condition of ageing

In the unmodified condition, the acicular eutectic Si particles acted as internal stress raiser in the microstructure and provided a crack initiation sites. The nucleation of sub-surface crack and their propagation to the surface becomes delaminating on worn surfaces. The elemental sodium modifier changed the microstructure from acicular (large plates with sharp sides and ends) to fibrous (with a fine, apparently globular morphology) structure. The change in the morphology of eutectic Si reduced the stress concentration at Al/Si interface and delaminating on the worn surfaces leading to a higher hardness upon heat treatment (Lee *et al*, 2012; Zhang *et al*, 2005; Leo and Cerri, 2003; Ernest, 2006).

The result of STAT (hardness value of 4.2HRF) is lower than the values obtained for DTAT in all ageing condition except at DTAT 120-5 h, which is similar to the results elsewhere (Abdulwahab, 2011; Waterloo *et al*, 2001; Risanti *et al*, 2009). The reason is probably because in the DTA treatment, finer dispersion of GP zones and Precipitates occurred.

4.2.1.2 Double-Thermal Ageing (DTAT)-T7 treatment

The result in Table 4.1 shows that the hardness increases as ageing time increases up to 3 h i.e. peak hardness of 6.7 HRF. Beyond this peak hardness, the value of hardness decreased with increasing ageing time.

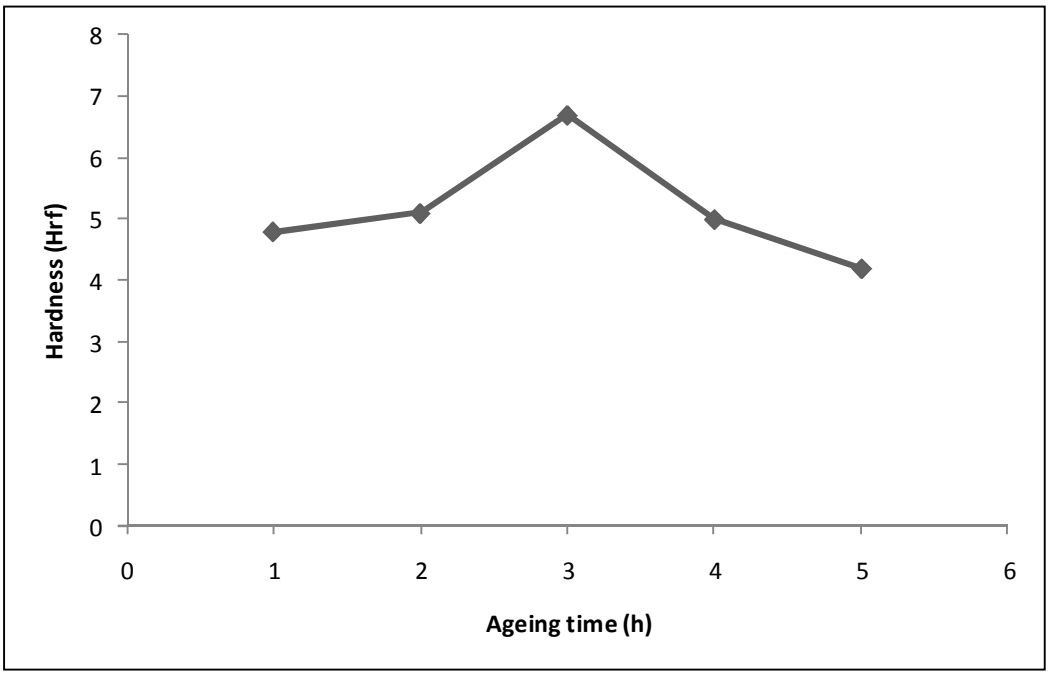


Figure 4.2: Variation of hardness with ageing time of Al-Si-Mg alloy after DTAT at 90^{o}C

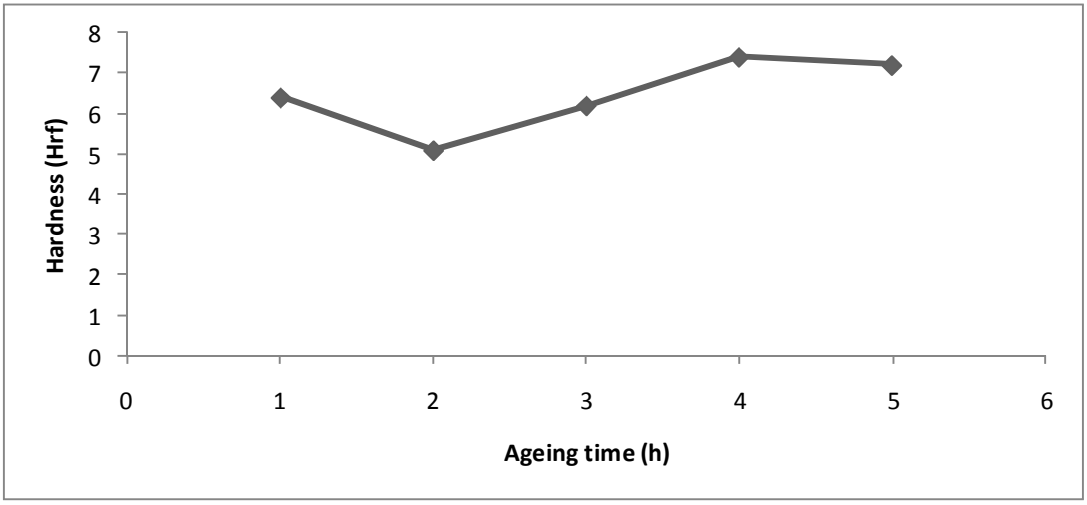


Figure 4.3: Variation of hardness with ageing time of Al-Si-Mg alloy after DTAT at 105^{o}C

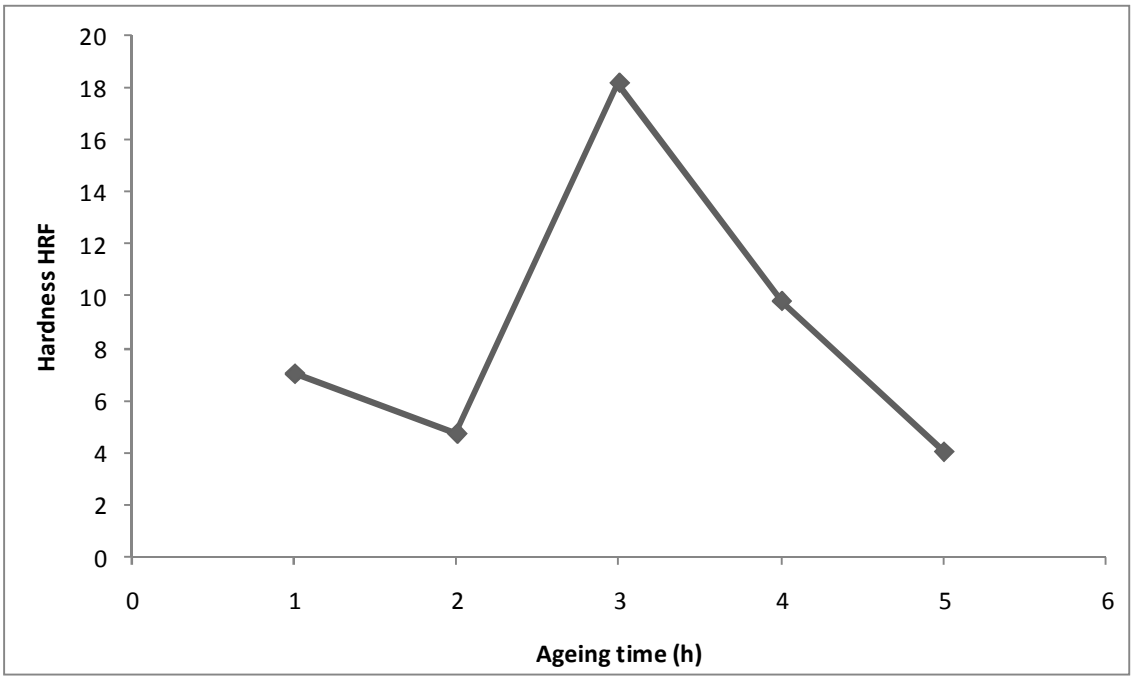


Figure 4.4: Variation of hardness with ageing time of Al-Si-Mg alloy after DTAT at 120^{o}C

The reasons for the increase in hardness can be as a result of an increase in the size and density of clusters in pre-aged microstructure. Usually, after solution at a sufficiently high temperature followed by quenching to room temperature, there will be a supersaturation of vacancies and alloying element leading to formation of the vacancy-rich clusters (VRC) (Waterloo *et al*, 2001).On subsequent artificial ageing, the clusters (β'' nuclei) produced by pre-ageing slower the process of natural ageing and accelerate the precipitation of β'' phase during subsequent artificial ageing (Hong *et al*, 2006).The reduction in hardness resulting from pre-ageing at 90^{o}C can be attributed to lower density of small hardening precipitates.

The result of DTAT in almost all ageing condition is higher compared to the STAT result of 4.2 HRF, which is similar to the results (Abdulwahab, 2011; Waterloo *et al*, 2001).

The difference in hardness at lower pre-ageing time for example DTAT at 105^{o}C after 3 and 4 h was 6.2 HRF and 7.4 HRF respectively. The difference may be that the incoherent precipitates appeared in the early hours of (3 h) and dissolve later probably due to diffusion of the precipitates and homogenization of the matrix. However, since diffusion /precipitation processes are slower at lower temperatures than higher temperatures, the precipitates appeared in the aluminium matrix only after higher ageing time (Callister, 1997; Abdulwahab, 2011).

The increase in hardness with ageing time when the Al-Si-Mg alloy was pre-aged at 120^{o}C was rapid with the peak hardness (18.2 HRF) at 3 h ageing time. At this pre-ageing temperature, the heat treatment might have resulted into a fine $Al_{12}Mg_{17}$, AlFeSi, Al_8Mg_3, $FeSi_6$ strengthening phases which are coherent along with the semi-coherent clusters. The alloy at this peak ageing temperature and time produces hardness value that is attributed to formation of Mg_2Si and other strengthening phases as observed by (Abdulwahab, 2011). This structure however indicates a spheroidized structure of silicon eutectics in the matrix of aluminium and the grain sizes are smaller and coherent with the matrix. That is the solute atoms form clusters which served as barrier to the movement of dislocation, and hence the higher hardness was obtained. This agrees with the work of several other researchers (Hong *et al*, 2006; Wang *et al*, 2008; Zhen and Kang, 1997; Abdulwahab, 2011).

Comparing of peak hardness values as a result of pre-ageing at 105^{o}C (i.e. 7.4 HRF at 4 h of ageing) and 120^{o}C (i.e. 18.2 HRF at 3 h of ageing), show that at the high ageing temperature, the alloy is expected to develop hardness at shorter ageing time because of the

faster rate of precipitation of the second phase particles. With the presence of the particles of the second phase precipitates, solute atoms tend to increase grain boundaries and higher hardness is expected (Dieter, 1987).

4.2.1.3: Comparative study between DTAT, STAT and as-cast Al-Si-Mg alloy studied

From the hardness results and discussions made, it is obvious that heat treatment have increased the hardness of this alloy under study. The DTAT treatment gave the alloy a higher hardness compared with the STAT treatment. In the DTAT treatments considered in this research, the DTAT at 120^{o}C for 3 h of ageing gave the alloy a higher hardness and may as well be adopted in substitute for the conventional STAT treatment of ageing at 180^{o}C for 2 h.

4.2.2 Correlation between Microstructures, Hardness and Corrosion Characteristics of Al-Si-Mg alloys

The as-cast microstructure as shown (Plate 5a) consists of α-aluminium solid solution with the flaky eutectic silicon phase. Modification treatment has changed the eutectic silicon phase to fibrous (Plate 5b). Within the α-aluminium solid solution, the elements are indicated by the EDS (Plates 1-4). This possibly indicates phases like Mg_2Si, $Al_{12}Mg_{17}$, AlFeSi, and $Al_8Mg_3FeSi_6$ can be said to be present in the thermally treated alloy. Considering Plates 3 and 4 i.e. microstructure of as-cast and STAT samples, it is obvious to conclude that there is an irregular distribution of eutectic phase formed which gives an understanding of the lower hardness obtained at this stage. The DTAT treatment gives

some microstructure with a better dissolution of the intermetallic (white phase) and the α-aluminium solid solution (black phase). This implies that the DTAT treatment has modified the microstructure of the Al-Si-Mg alloy studied, hence increasing the hardness and corrosion characteristics of the alloy within the time considered.

The corrosion resistance of DTAT Al-Si-Mg alloys seem to be strongly associated not only with the extensive distribution of eutectic, which is dependent on the interdendritic spacing, but also with the fineness of the eutectic interphase spacing as observed in this research.

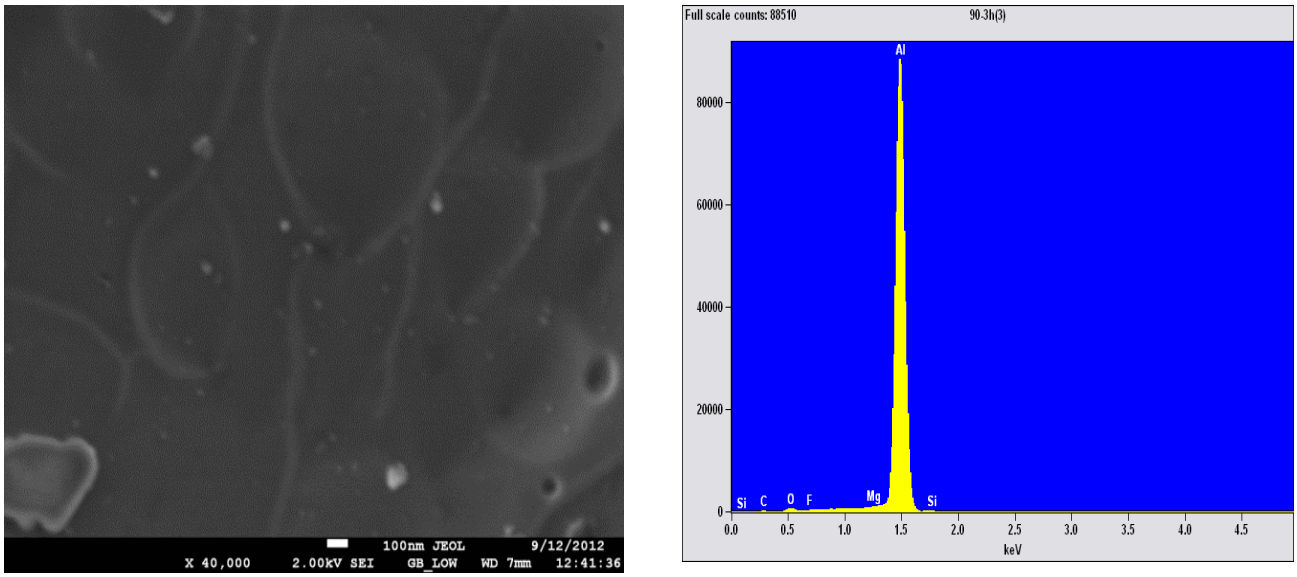


Plate 1: SEM microstructure and EDS spectrum of Al-Si-Mg alloy after pre-ageing at 90^{o}C for 3 h.

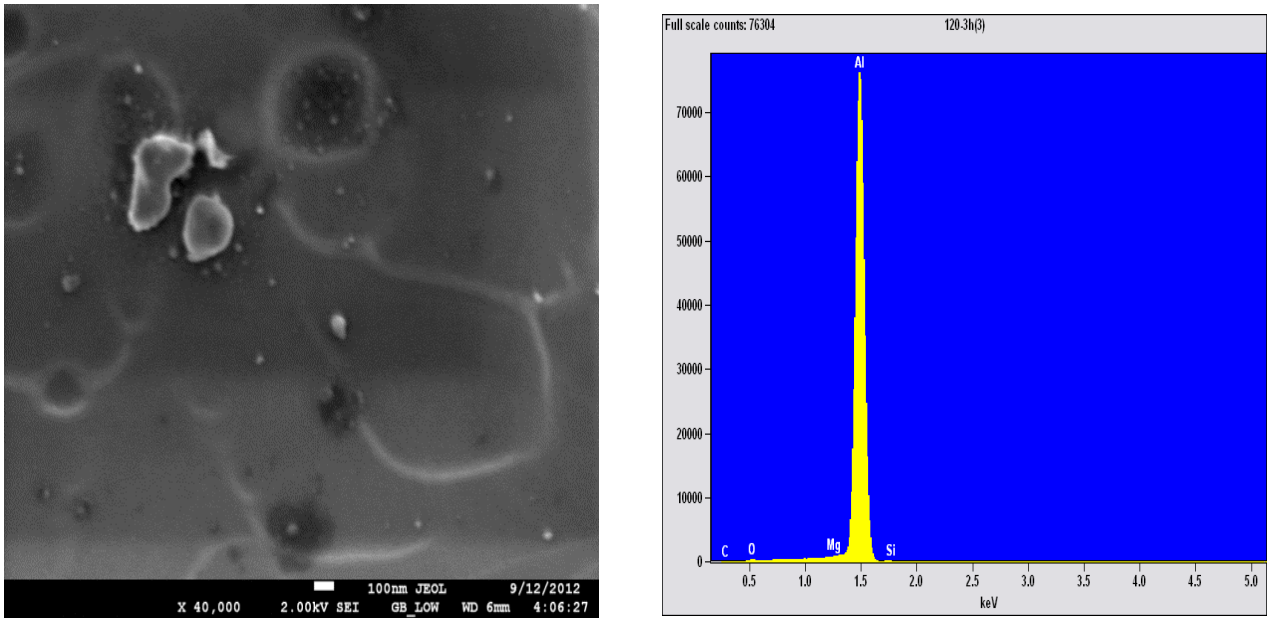


Plate 2: SEM microstructure and EDS spectrum of Al-Si-Mg alloy after pre-ageing at 120^{o}C for 3 h

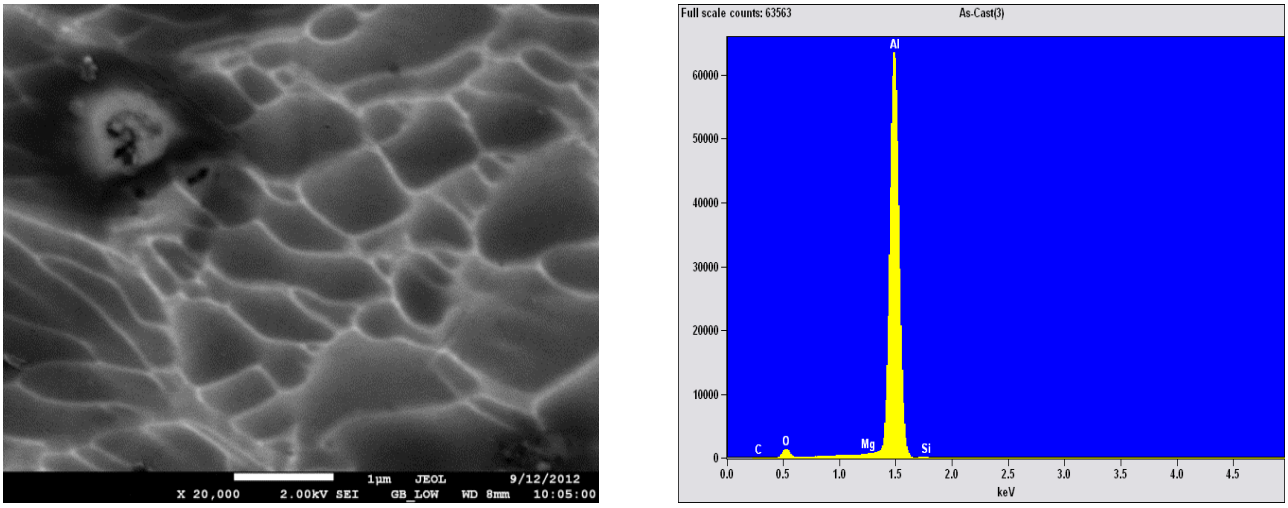
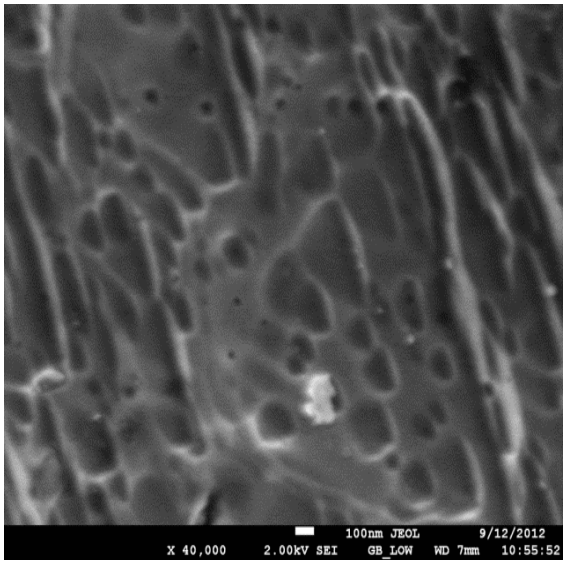


Plate 3: SEM microstructure and EDS spectrum of as-cast Al-Si-Mg alloy



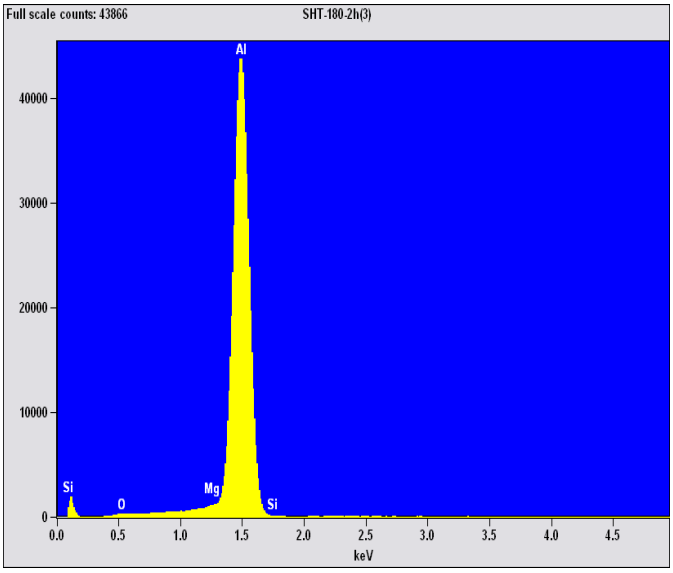


Plate 4: SEM microstructure and EDS spectrum of Al-Si-Mg alloy after STAT-T6 treatment at 180^{o}C for 2h

4.2.3 CORROSION CHARACTERISTICS AND THERMAL AGEING TREATMENT

4.2.3.1 Weight loss

The corrosion rates of Al-Si-Mg alloy in various heat treatments are as shown in Table 4.6. From the results obtained, the as-cast Al-Si-Mg alloy has the highest corrosion rate.

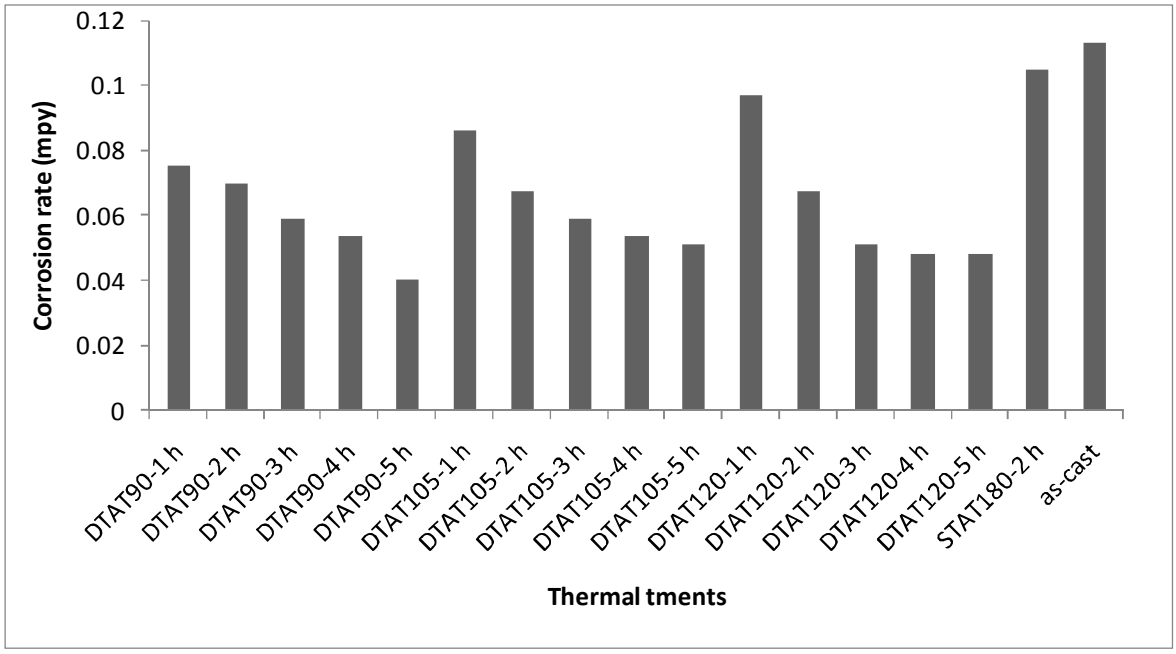


Figure 4.5: Corrosion characteristics of Al-Si-Mg alloy under different condition of ageing with the as-cast

This implies that the corrosion susceptibility of this alloy is greatly dependent on the heat treatment. Also, DTAT-T7 treatment has demonstrated a remarkable decrease in the corrosion rate than STAT-T6 samples at all the ageing time considered. This agrees with the works (Feng *et al*, 2008; Reda *et al*, 2008; Uhlenhaut *et al*, 2009; Abdulwahab, 2011).

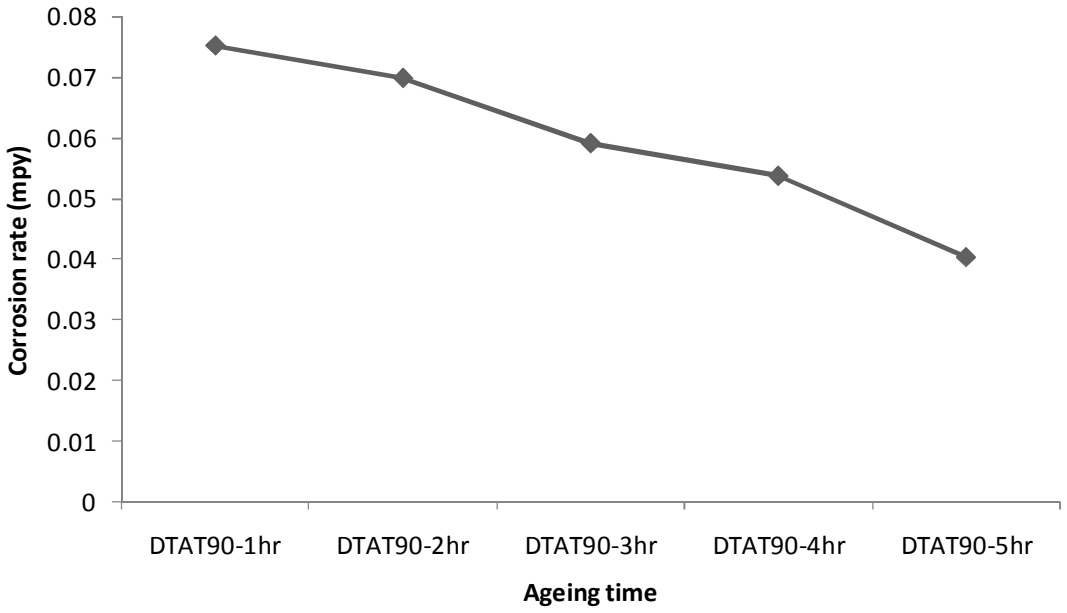


Figure 4.6: Variation of corrosion rate with ageing time for DTAT-T7 at 90^{o}C

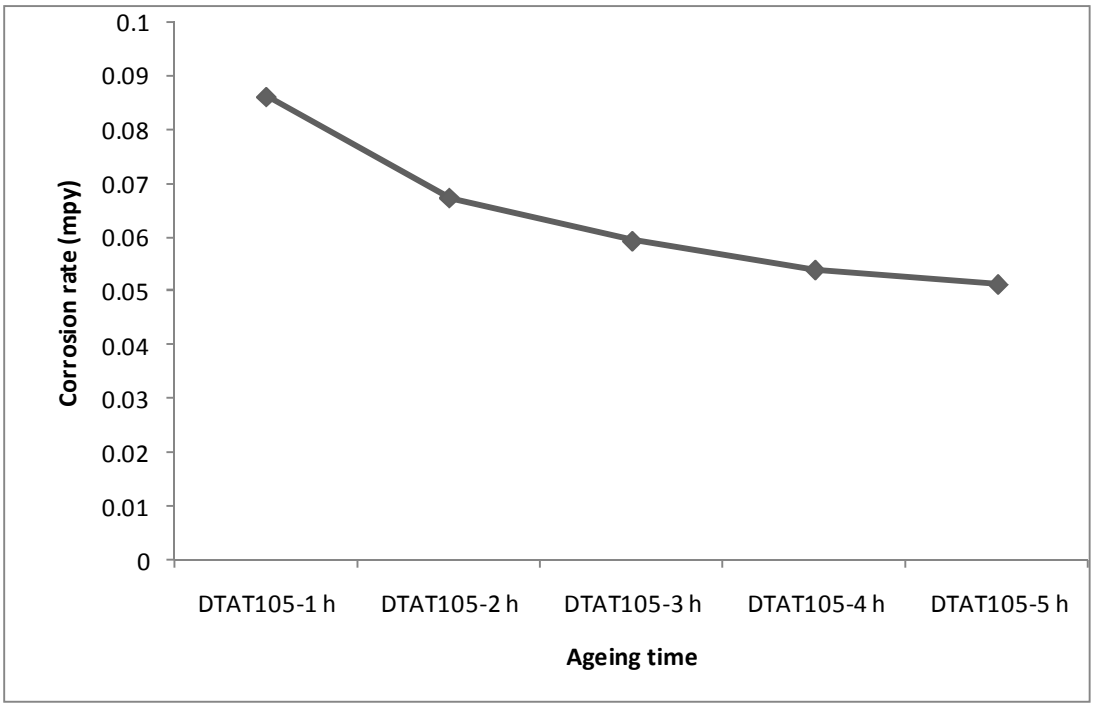


Figure 4.7: Variation of corrosion rate with ageing time for DTAT-T7 at 105^{o}C

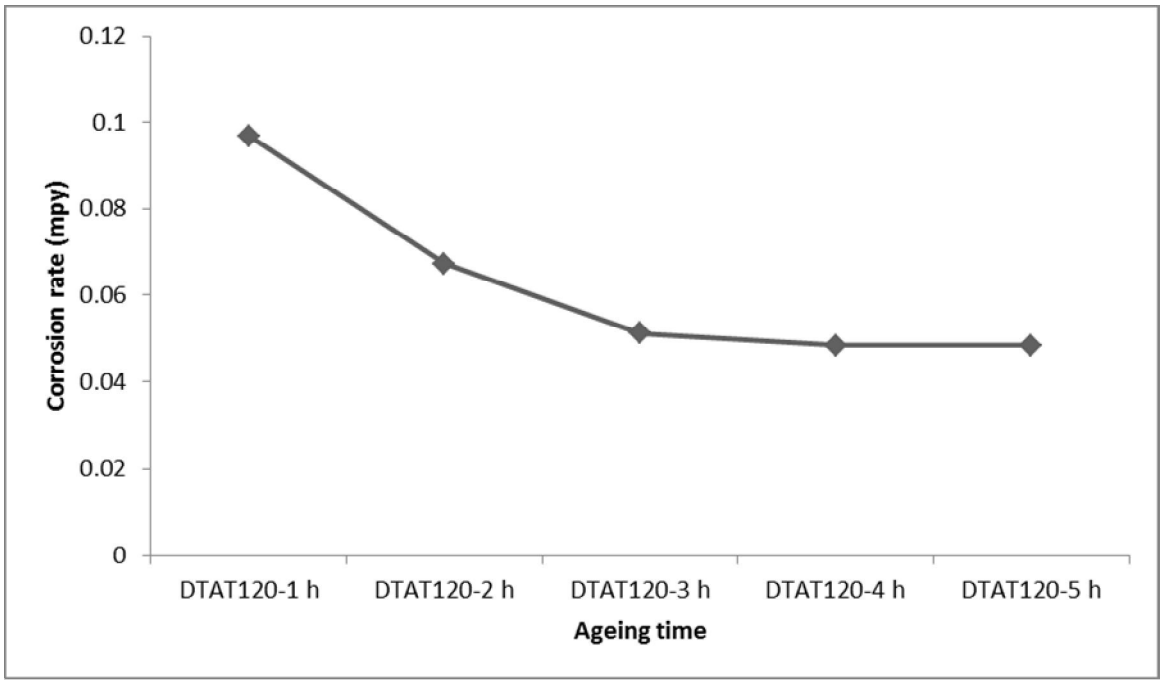


Figure 4.8: Variation of corrosion rate with ageing time for DTAT-T7 at 120^{o}C

The reason for the higher corrosion resistance of the DTAT samples is that DTAT promotes coarse precipitates of the equilibrium phase β in the grains and sub-grains boundaries, while maintaining a fine distribution of β^{1} in the grain interiors. These coarse intermetallic particles then act as hydrogen trapping sites, locally reducing the hydrogen concentration in the matrix around the grain boundary. Similar results have been obtained elsewhere (Reda *et al*, 2008).

From the hardness measurement, it is expected that samples with higher HRF should have greater corrosion rate. At higher HRF, grain size of the sample is finer and such structures are more susceptible to corrosion than coarse ones, especially when the precipitate on the

grain boundaries of the alloy becomes coarser (Feng *et al*, 2008; Abdulwahab, 2011). But this did not hold for this work. Abdulwahab (2011) have shown that this is possible and may be attributed to the $Al_{13}Cr_4Si_4$ phase which usually enhances strength/hardness and precipitate more as the ageing time increases, thus reducing the corrosion rate.

The corrosion rate of DTAT decreases with an increase in ageing time. Usually, the DTAT treatment is a two –step ageing treatment. During the first ageing process for increasing time, the phase of β^1 is precipitated within the grain. Then during the second ageing at a higher temperature, the β^1 precipitates coarsen and their density is reduced.

Feng et al, 2008 showed that the corrosion potential of the η-precipitate was negative with respect to that of the alloy base at its adjacent periphery, and its corrosion current density was much greater, indicating that the η precipitate was more sensitive to corrosion than the alloy base. The preferential corrosion of the η precipitate at the grain boundary is in agreement with the electrochemical behaviours of the precipitate of η and the alloy base. Therefore, as the Al-Si-Mg alloy is immersed in the 3.5% NaCl solution, the β precipitates will act as anodic zones and be preferentially attacked. However, the alloy base at their adjacent periphery is protected as a cathodic zone. The precipitates of βare distributed continuously at the grain boundaries of the Al-Si-Mg-T6 alloy. Therefore, there exists an active corrosion path resulting from the galvanic reaction between the anodic precipitates of β at the grain boundary and the alloy base at their adjacent periphery, which leads to its greatest susceptibility to corrosion.

The difference in corrosion rate between the DTAT samples at the same time, like DTAT at 90°C/1 h (0.07532 mpy) and DTAT at 105°C/1 h (0.08608 mpy) could be that as the precipitates of βat the grain boundaries are distributed discontinuously in the Al-Si-Mg alloy, corrosion path exists in these alloys and their susceptibility to corrosion is decreased. Also, when the spacing between the β precipitates at the grain boundaries of the alloy is largest; its susceptibility to corrosion is decreased.

4.2.3.2 Linear Polarisation Corrosion

Tables 4.9 - 4.11 give the values of kinetic corrosion parameters as the corrosion potential E_{corr}, corrosion current density $I_{corr\ and}$ Tafel slopes (b_c and b_a) for the corrosion of as-cast, STAT and some DTAT Al-Si-Mg alloy in 3.5% NaCl solution. The corrosion current densities were estimated from the Tafel extrapolation of the cathodic and anodic curves.

The as-cast Al-Si-Mg alloy has the highest current density and corrosion rate followed by the STAT samples, then DTAT sample in all the pre-ageing conditions considered. From the linear polarisation resistance value, R_p, the DTAT temper has the highest R_p and corrosion potential (E_{corr}) followed by the STAT temper and lastly the as-cast samples. I.e. DTAT 90°C 1 h (R_p is 4837.6 Ω and I_{corr} is 0.00000117 A/cm^2), DTAT 105°C 1 h (R_p is 3927.3 Ω and I_{corr} is 0.00000172 A/cm^2), DTAT 120^{0}C 1 h (R_p is 17041 Ω and I_{corr} is 0.000000386 A/cm^2), STAT 180°C 2 h (R_p is 3311.3 Ω and I_{corr} is 0.00000624 A/cm^2) as-cast (R_p is 1247.2 Ω and I_{corr} is 0.00000758 A/cm^2). Generally, an increase in polarisation resistance, R_p leads to a decrease in the current density, I_{corr}. The increase in R_p generally suggested an improvement in the corrosion resistance of the alloy as a result of the temper

treatment. The DTAT treatment can be said to have improved the corrosion resistance of the Al-Si-Mg alloy studied. This is in agreement with the previous studies (Abdulwahab, 2011).

From Figures 4.9-4.11, the anodic and cathodic branches changes with a change in the temper treatment were presented for some thermal treated samples.

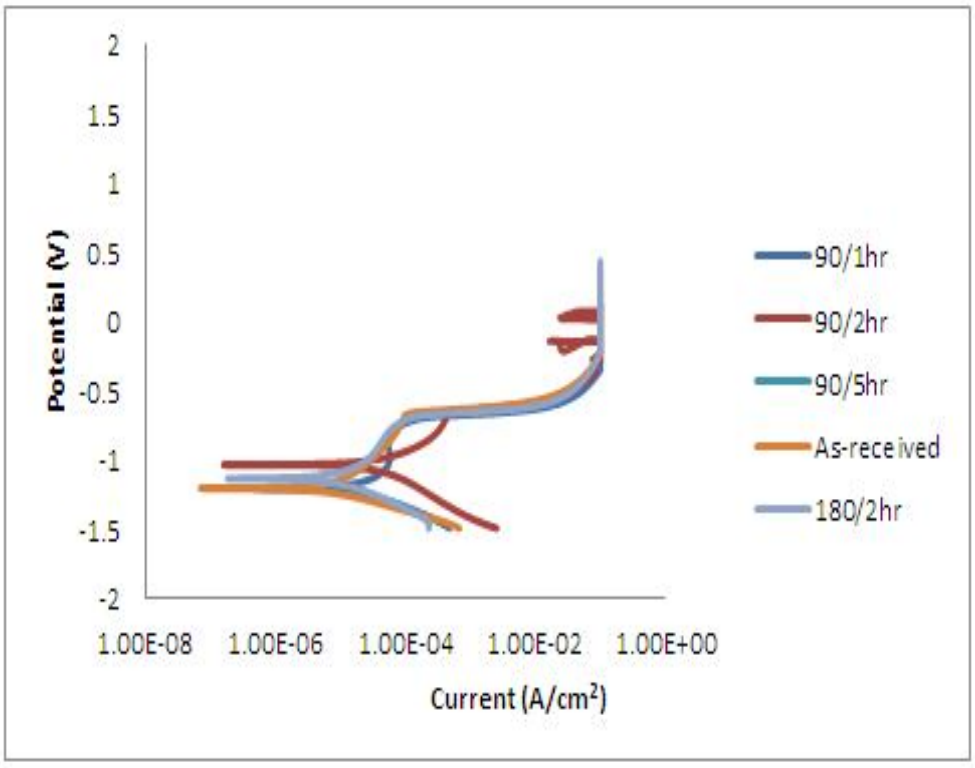


Figure 4.9: Linear polarisation of as-cast, STAT and DTAT Al-Si-Mg alloy after pre-ageing at 90°C

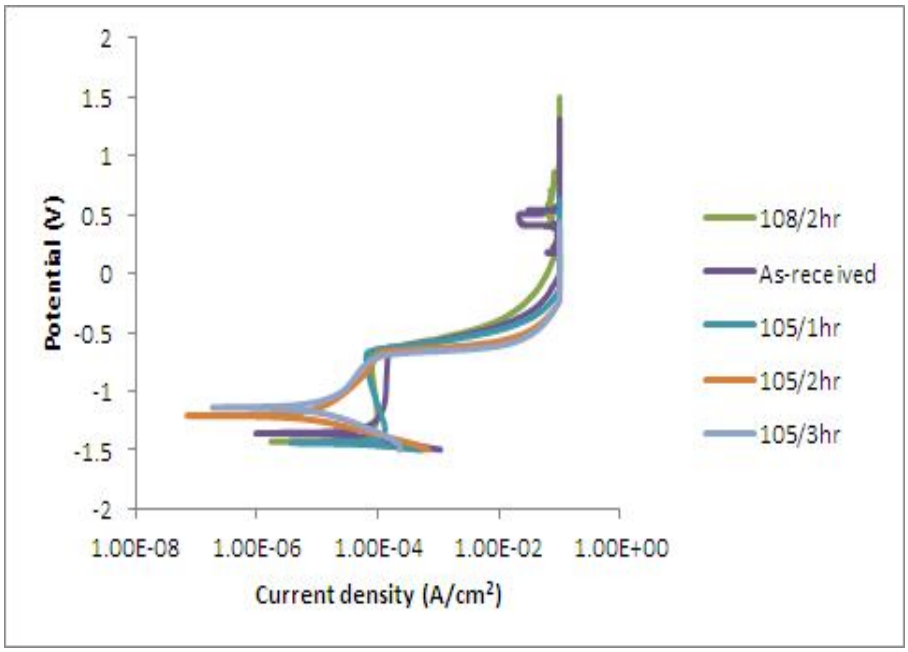


Figure 4.10: Linear polarisation of as-cast, STAT and DTAT Al-Si-Mg alloy after pre-ageing at 105°C

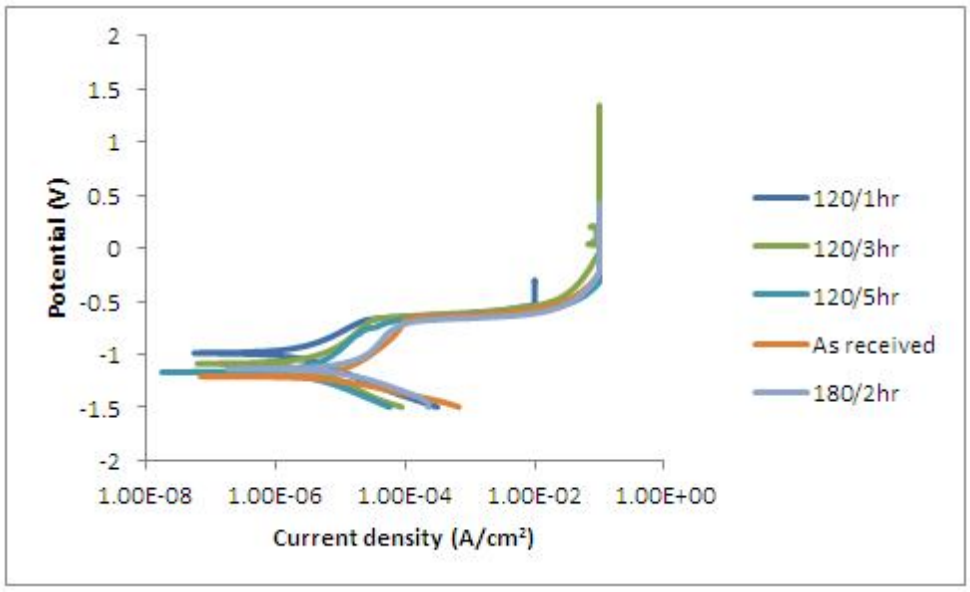


Figure 4.11: Linear polarisation of as-cast, STAT and DTAT Al-Si-Mg alloy after pre-ageing at 120°C

This shows that the temper treatment reduces anodic dissolution and retards the hydrogen evolution reaction. The current densities (corrosion rate) and their corresponding corrosion potentials are also shown in the figures. Such result permit to observe that the corrosion rate is very similar for all the examined alloy. This is so because such alloys were solidified in similar conditions of cooling rate and as a consequence a same order of magnitude of dendritic spacing should be expected. Osorio *et al*, 2007 have shown that the dendritic spacing plays an important role on the corrosion resistance of binary alloys. The temper at DTAT 120-3 h showed the lowest corrosion rate for the period of time considered in this experiment. This is possible because grain boundaries are often more susceptible to corrosion than the grain interior because of the heterogeneity associated with the grain boundaries. It is expected that samples with higher corrosion have pronounced grain boundaries, as such higher hardness is expected for such sample as is the case in this research.

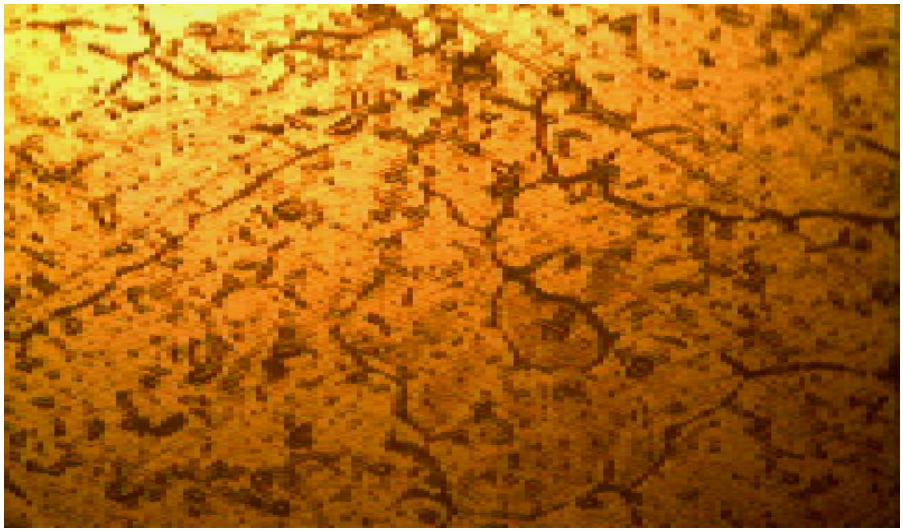


Plate 5a: Microstructure of unmodified Al-Si-Mg alloy showing silicon flakes within aluminium matrix (x300)

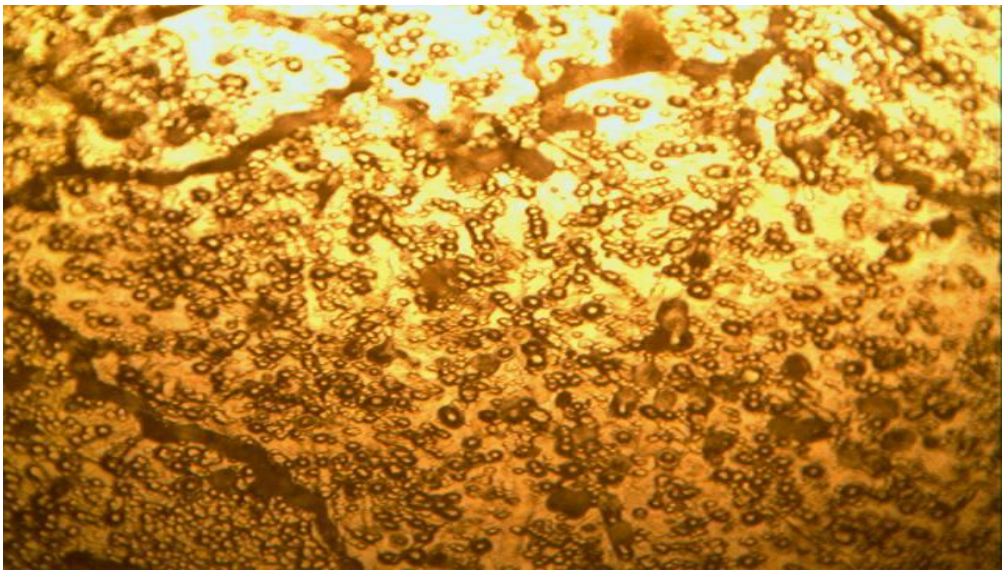


Plate 5b: Microstructure of elemental sodium modified Al-Si-Mg alloy showing the breakdown/spheroidization of silicon flakes (x300)

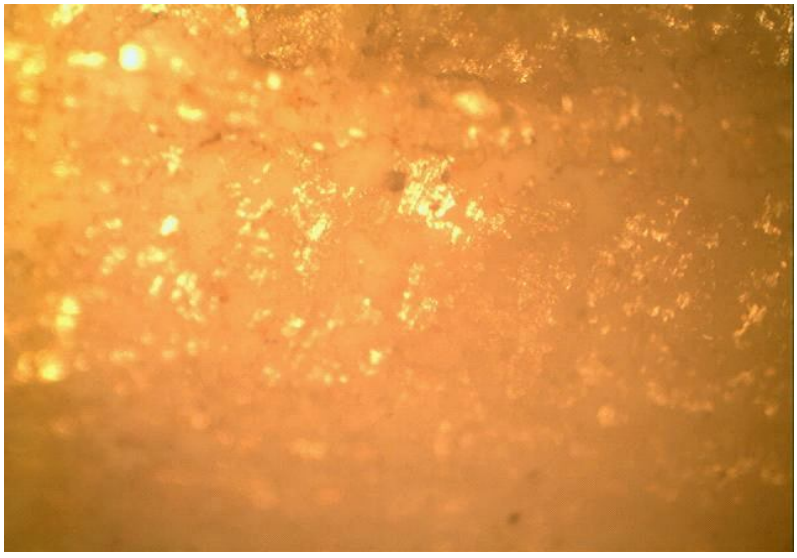


Plate 6a: As- Corroded microstructure of DTAT-90/3 h Al-Si-Mg alloy after 30 days immersion in simulated sea water (x300)

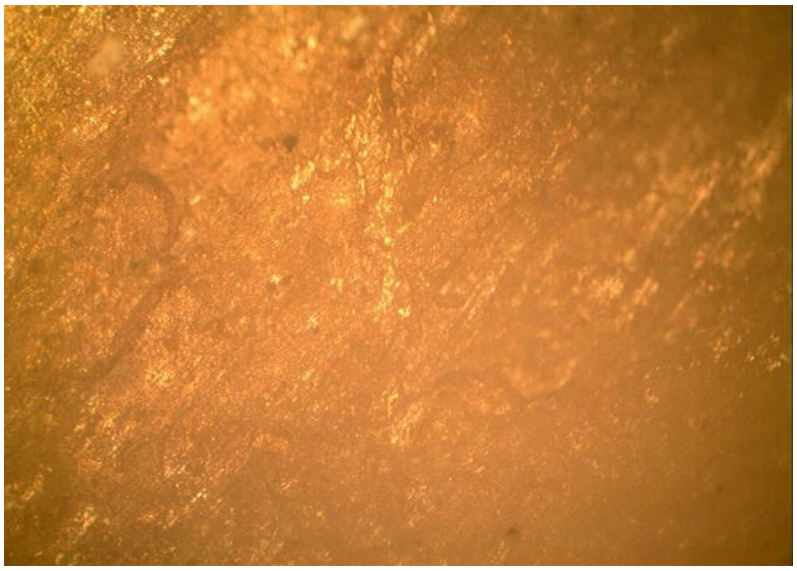


Plate 6b: As- Corroded microstructure of DTAT-105/3 h Al-Si-Mg alloy after 30 days immersion in simulated sea water (x300)

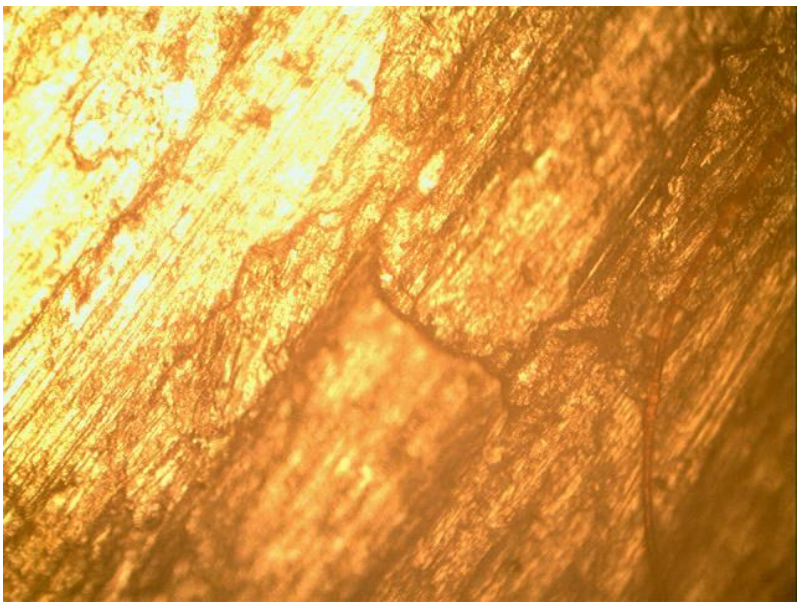


Plate 6c: As- Corroded microstructure of DTAT-120/3 h Al-Si-Mg alloy after 30 days immersion in simulated sea water (x300)

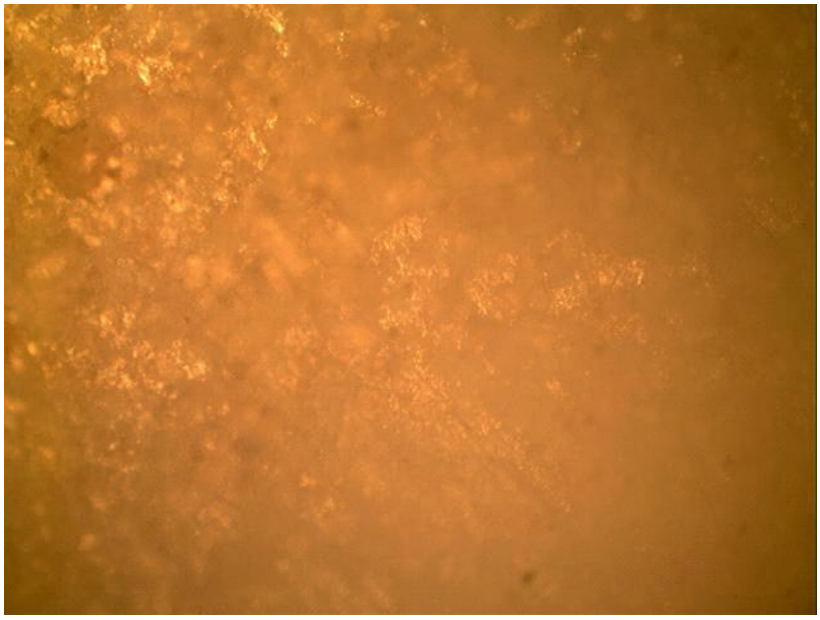


Plate 6d: As- Corroded microstructure of DTAT-180/2 h Al-Si-Mg alloy after 30 days immersion simulated sea water (x300)

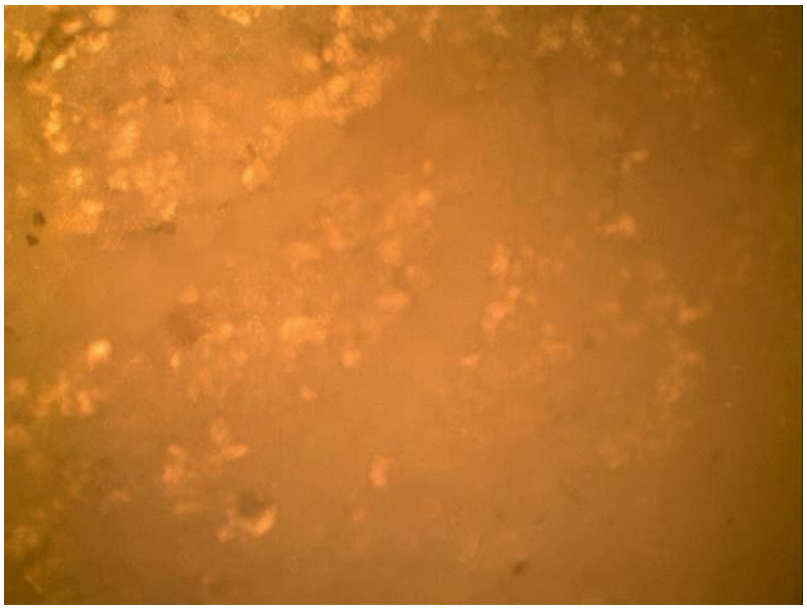


Plate 6e: As- Corroded microstructure of as-cast Al-Si-Mg alloy after 30 days immersion in simulated sea water (x300)

CHAPTER FIVE

SUMMARY, CONCLUSION AND RECOMMENDATIONS

5.1 Summary

The effect of pre-ageing conditions on the hardness and corrosion characteristics of double-thermally aged chill cast Al-Si-Mg alloys in simulated sea water environment has been studied. The temper conditions are DTAT at 90^{o}C, 105^{o}C and 120^{o}C with variable pre-ageing time. These were compared with the conventional treatment of this alloy (STAT). The as-cast Al-Si-Mg alloy was also studied. Within the α-aluminium solid solution, the elements are indicated by the EDS. This possibly indicates phases like Mg_2Si, $Al_{12}Mg_{17}$, AlFeSi, and $Al_8Mg_3FeSi_6$ which can be said to be present in the thermally treated alloy. The hardness of the Al-Si-Mg alloy was observed using the Rockwell-F scale hardness tester, while the corrosion characteristics was evaluated using weight loss and linear polarisation techniques in 3.5% NaCl solution.

From the results (Figure 4.1), DTAT samples showed better hardness value as compared with the STAT and as-cast samples. The DTAT treatment has increased the alloy by more than a 100% in two temper conditions i.e. DTAT at 120^{o}C for 3 h (with a hardness value of 18.2 HRF) and DTAT at 120^{o}C for 4 h (with a hardness value of 9.8 HRF) as compared with the conventional STAT treatment (with a hardness value of 4.2 HRF).

The corrosion of the DTAT treated samples in all temper conditions in the simulated sea water showed a higher improvement in corrosion resistance than the as-cast and conventional STAT alloy. From the OPM results of as-corroded samples, it is obvious that

the type of corrosion that occurred in this alloy is pitting/uniform corrosion. The hardness results of some selected samples after weight loss corrosion in simulated sea water also showed a decrease in hardness value as compared with its hardness before corrosion attack. The linear polarisation of some of the thermally treated samples demonstrated a higher corrosion potential and linear polarisation resistance with lower current density as compared with the as-cast and STAT samples.

5.2 Conclusion

From an energy savings point of view, research has been focusing on examining the possibility of shortening the heat treatment cycle, especially reducing the solutionizing and ageing time without sacrificing mechanical properties to a great extent (Ma *et al*, 2006). In this research, the variation in pre-ageing conditions of the DTAT samples has greatly improved the hardness value with more than a 100% as a result of a low temperature ageing at 120^{o}C for 3 h and 4 h. However, significant results have been obtained with higher corrosion resistance in the DTAT-temper condition than the STAT temper. In line with the above, the following conclusions are made;

1- DTAT treatments with varying pre-ageing thermal treatment have been shown as one of the possible ways to improve hardness value and corrosion resistance of Al-Si-Mg alloy within the studied pre-ageing temperatures and times.

2- The peak hardness value of 18.2 HRF was achieved from DTAT treatment comprising of a low temperature ageing at 120^{o}C for 3 h of ageing, followed by ageing at 180^{o}C for 2 h. The hardness obtained at 180^{o}C for 2 h of ageing (4.2

HRF) is also lower than other DTAT treatment temperatures like DTAT at 90^{o}C for 1, 2, 3 and 4 h of ageing, also DTAT at 105^{o}C for 1, 2, 3, 4 and 5 h of ageing and DTAT at 120^{o}C for 1, 2, 3, and 4 h of ageing for the alloys considered in this study.

3- The improvement of hardness with the DTAT treatment can be attributed to the finer dispersion of precipitates obtained as a result of the low temperature ageing, which was further retained and fully transformed to finer particles at higher ageing temperature and time.

4- The results of weight loss of Al-Si-Mg alloy in simulated sea water environment has shown that the corrosion resistance of DTAT Al-Si-Mg alloy has been enhanced significantly as compared to those observed in the STAT temper condition.

5- From the results of corrosion rate determined from weight loss of coupons, it was shown that the corrosion rate decreases at all pre-ageing temperatures and time. The corrosion of the DTAT samples in simulated sea water showed higher corrosion resistance than the STAT samples.

6- Results from linear polarization had a better corrosion resistance for the DTAT samples as compared with the STAT and as-cast Al-Si-Mg alloy and DTAT 120^{o}C for 3 h indicated the highest corrosion rate.

5.3 RECOMMENDATIONS FOR FURTHER WORKS

1- The effect of DTAT on Al-Si-Mg alloy using other casting technique like investment die casting and permanent mold casting should be studied.

2- TEM study of the crystal orientation and GP zones of the alloy is recommended.

3- XRD of this alloy after thermal treatment is also recommended for further study.

REFERENCES

Abdulwahab, M. (2007). *The Effect of Chromium and Manganese on the Mechanical Properties and Corrosion Resistance of Al-Si-Fe Alloy in 0.5M HCl Solution.* (Unpublished Master's thesis). Department of Metallurgical and Materials Engineering, Ahmadu Bello University, Zaria, Nigeria.

Abdulwahab, M., Madugu, I.A., Yaro, S.A., Popoola, A.P.I. (2011a). Degradation Behaviour of High Chomium Sodium-Modified A356.0-Type Al-Si-Mg Alloy in Simulated Seawater Environment. *Journal of Minerals and Materials Characterization and Engineering*, 10(6), 535-551.

Abdulwahab**,** M., Madugu, I.A., Yaro, S.A., Hassan, S.B., and Popoola, A.P.I. (2011b). Effects of Multiple-Step Thermal Ageing Treatment on the Hardness Characteristics of A356.0-type Al-Si-Mg Alloy. *Materials and Design,* 32(3), 1159-1166.

Abdulwahab, M. Madugu, I.A. Yaro, S.A. and Popoola, A.P.I. (2012). Effects of Temper Conditions and Step-quenching-Ageing on the Hardness Characteristics and Yield Strength of A356.0-type Al-Si-Mg Alloy. *Silicon,* 4(2), 137-143.

Abdulwahab, M. (2011). *Effect of Multiple-Step Thermal Ageing Treatment on the Hardness and Corrosion Characteristics of A356.0-Type Al-Si-Mg Alloy*. (Unpublished Doctoral dissertation). Department of Metallurgical and Materials Engineering, Ahmadu Bello University, Zaria, Nigeria.

ASM. (1978). *Source Book on Selection and Fabrication of Aluminium Alloys.* American Society of Metals Publication.

Auwal, K. (2012). *Linear Polarisation Resistance Monitoring*. Advance Corrosion Engineering, Lecture note, MMEN 806, Department of Metallurgical and Materials Engineering, Ahmadu Bello Universirty, Zaria.

Avner, S.H. (1997). *Introduction to Physical Metallurgy.* (2nd ed.), Tata McGraw-Hill Publishing Company limited, New Delhi.

Aye, S.W.H., Lwin, K.T., Khine, W.W.K. (2008). *The effect of ageing treatment of aluminium alloys for fuselage structure-light aircraft.* Proceeding of world academy of Science Engineering and Technology, Vol. 36.

Bangyikhan, K. (2005).*Effect of Oxide Film, Fe-rich phase, Porosity and their Interactions on Tensile Properties of Cast Al-Si-Mg Alloys*. (Unpublished Doctoral dissertation). University of Birmingham, Birminghan).

Birol, Y. (2009). Response to Artificial Ageing of Dendritic and Globular Al-7Si-Mg Alloys. *Journal of Alloys and Compounds*, 484, 164-167.

Choundary, R.B. (2007). *Materials Science and Metallurgy*. khanna Publishers, NaiSarak, Delhi.

Callister, W.D. (2001). *Fundamentals of Materials Science and Engineering an interactive* John Wiley and Sons Inc, United States.

Dirras,G.F., Donnadieu. P., Douin. J. (2010). *Dislocation/Precipitate interaction mechanisms in 6xxx aluminium alloys*. 76, 62-68. Ernst, F. (2006). *Precipitation Hardening of Al-Si-Mg Alloys.* Materials Laboratory III, Spring Semester Lecture Note, EMSE-290.

Fracasso, F. (2010). *Influence of Quench Rate on the Hardness obtained after Artificial Ageing of an Al-Si-Mg Alloy*. (Unpublished Doctoral dissertation). Jonkoping Institute of Technology, Tekniska Hogskolan.

Feng, L.J., Wei, P.Z., Xing, L.C., Qiang, J.Z., Jing, C.W., Qiao, Z.Z. (2008). Mechanical Properties, Corrosion Behaviors and Microstructures of 7075 Aluminium Alloy with various Ageing Treatments. *Transactions of Nonferrous Metals Society of China*, 18, 755-762.

Haghshenas, M., Hanzaki, A.Z., Varzaneh, S.M.F. (2008). The Effects of Thermo- Mechanical Parameters on the Microstructure of Thixocast A356 Aluminium Alloy. *Material Science and Engineering A*, 480, 68-74.

Hassan, S.B., Aigbodion, V.S. (2009). The Effect of Thermal Ageing on Microstructure and Mechanical Properties of Al-Si-Fe/Mg Alloys. *Journal of Alloys and Compounds*, 486, 309-314.

Hong, L., Yang, C., Gang, Z., Ming, L.C., Liang, Z. (2006). Effect of Pre-Ageing on Precipitation Behavior of Al-1.29Mg-1.22Si-0.68Cu-0.69Mn-0.3Fe-0.2Zn-0.1Ti Alloy, *Transactions of Nonferrous Metals Society of China.*16, 917-921.

International Aluminum Institute. (2008). Heat Treatment of Aluminium Alloys. www.key-to-metals.com, internet link.

Juang, S.H., Wu, S.M. (2008). Study on the Mechanical Properties of A356 Alloys enhanced with Preformed Thixotropic Structure. *Journal of Marine Science and Technology*. 16(4), 271-274.

Jacobs M. (1999). *Precipitation Hardening.* TALAT Lecture:Interdisciplinary Research Centre in Materials. The University of Birmingham, UK , 2-10.

Joseph, U.I (2009). *The effect of Ageing Time on the Corrosion Susceptibility of Al-2.1%Si-0.7%Fe-0.4%Cr and Al-2.1%Si-0.7%Fe Alloy in HCl solution.* (Unpublished Final year project). Department of Metallurgical and Materials Engineering, Ahmadu Bello University, Zaria, Nigeria.

Kumar,G., Hegde, S.B., Prabhu, N. (2007). Heat Transfer and Solidification Behavior of Modified A357 Alloy. *Journal of Materials Processing Technology*. 182, 152-156.

Khomamizadeh, F., Ghasemi, A. (2004). Evaluation of Quality Index of A356 Aluminium Alloy by Microstructural Analysis. *Scientia Iranica.* 11(4) 386-391.

Kliauga, A.M., Vieira, E.A., Ferrante, M. (2008). The influence of impurity level and Tin addition on the Ageing Heat Treatment of The 356 Class Alloy. *Materials Science and Engineering A*. 480, 5-16.

Li, Y.J., Brusethaug, S., Olsen, A. (2006). Influence of Cupper on the Mechanical Properties and Precipitation Behavior of AlSi7Mg0.5 Alloy during Ageing Treatment. *Scripta Manterilia*, 54, 99-103.

Leo, P., Cerri, E. (2003). *Silicon Particle Damage in a Thixocast A356 Aluminium Alloy.* 21, 1.

Lozano, J.A., Voort, G.V. (2010). Using Microstructural Analysis to solve practical problems. *Buehler*, 5, 1.

Ma, S. (2006). *A Methodology to predict the effects of Quench rates on Mechanical Properties of Cast Aluminium Alloys* (Unpublished Doctoral dissertation). Worcester Polytechnic Institute, Materials Science and Engineering.

Ma, S., Maniruzzaman, M., Mackenzie, D.S., Sisson, R.D. (2006). *A Methodology to predict the effects of Quench rates on Mechanical Properties of Cast Aluminium Alloys*. Worcester Polytechnic Institute, Worcester.

Narayan, K.P., Ravishankar, B.N. (2003). Effect of Modification Melt Treatment on Casting/Chill Interfacial Heat Transfer and Electrical Conductivity of Al-13%Si Alloy. *Material science and engineering A,* 360 (293-298).

Osorie, W.R., Spinelli, J.E., Freire, C.M.A., Cardona, M.B., Garcia, A. (2007). The Roles of Al_2Cu and of Dendritic Refinement on Surface Corrosion Resistance of Hypoeutectic Al-Cu alloys immersed in H_2SO_4. *Material Science and engineering* A, 67(15) 176-183.

Perez, N. (2004). *Electrochemistry and Corrosion Science.* New York, Boston: Kluwer Academic Publishers.

Rashid, A. (2010). *The Treatment of Liquid Aluminium-Silicon Alloys.* Department of Metallurgical and Materials Engineering, MME 6203, Lecture 13, BUET, Dhaka.

Risanti, D.D., Yin, M., Rivera, D., Castillo, P.E.J., Zwaag, S.V. (2009). A Systematic Study of the Effect of Interrupted Ageing conditions on the Strength and Toughness development of AA6061. *Journal of Maternal Science and Engineering A,* 523, 99.

Reda, Y., karem, R.A., Elmahallawi, I. (2008). Improvements in Mechanical and Stress Corrosion Cracking Properties in Al-Alloy 7075 via Retrogression and Re-ageing. *Materials Science and Engineering A,* 485, 468-475.

Rawajfeh, A.E., & Qawabah, S.M.A. (2009). Investigation of Copper addition on the Mechanical Properties and Corrosion resistance of commercially pure Aluminium. *Emirates Journal for Engineering Research,* 14(6) 47-52.

Sun,Y., Baydogan, M., Cimenoglu, H. (1999). The effect of deformation before ageing on the wear resistance of an aluminium alloy.*Materials Letters*, 38(8) 221-226.

Svenningsen, G., Larsen, M.H., Nordlien, J.H., Nisancioglu, K. (2006). Effect of Thermo-Mechanical history on intergranular corrosion of extruded AlMgSi (Cu) model alloy. *Journal of corrosion science*, 48(12) 3970-3973.

Seifeddine, S. (2007). *The Influence of Iron on the Microstructure and Mechanical properties of Al-Si alloys.* School of Engineering:Jonkoping University.

Shaffer, J.P., Antolovich, S.D., Sanders, T.H., Warner, S.B., Sexena, A. (1999). *The Science and Design of Engineering Materials.* (2nd ed), McGraw-Hill.

Tash, M., Samuel, F.H., Mucciardi, F., Daty, H.W. (2007). Effect of Metallurgical Parameters on the Hardness and Microstructural Characterization of As-cast and heat treated 356 and 319 Aluminum alloys. *Journal of Material Science and Engineering A* 443(23) 185-188.

Uhlenhaut, D.J., Furrer, A., Uggowitzer, P.J., Loffler, J.F. (2009). Corrosion Properties of Glassy Mg70Al15Ga15 in 0.1M NaCl. *Journal of Intermetallics*, 25(17) 811-817.

Umaru, O.B. (2009). *The Effect of Ageing Time on the Tensile Properties of Cast Al-2.1%Si-0.7%Fe-0.4%Cr Alloys.* (Unpublished undergraduate project). Ahmadu Bello University, Zaria, Nigeria.

Wang, W., Zhang,X., Gao, Z., Jia, Y., Ye, L., Zheng, D., Liu, L. (2009). Influence of Ce addition on the microstructures and mechanical properties of 2519A aluminium alloy plate. *Journal of Alloys and Compounds*, 17, 39-47.

Waterloo, G., Hansen, V., Gjonnes, V., Skjervold, S.R. (2001). Effect of pre-deformation and pre-ageing at room temperature in Al-Zn-Mg-(Cu, Zr) alloys. *Materials science and engineering A*. 303(17) 226-233.

Wei, B.C., Chen, C.Q., Huang, Z., Zhang, Y.G. (2005). Ageing behaviour of Li containing Al-Zn-Mg-Cu Alloys. *Materials Science and Engineering A*. 280, 161-167.

Ye, Haizhi. (2003). An overview of the development of Al-Si-Alloy based Material for Engine Applications. *JMEPEG*, 12, 288-297.

Zhang, Y., Ma, N., Le, Y., Li, S., Wang, H. (2005). Mechanical Properties and Damping Capacity after Grain Refinement in A356 Alloy. *Materials Letter*, 59, 2174-2177.

Zhen, L., & Kang, S.B. (1997). The Effect of Pre-ageing on Microstructure and Tensile Properties of Al-Mg-Si Alloys. *Scripta Materialia*, 36 (10) 1086-1092.

Zhonwei, C., Jinshan, L., Wanqi, J., Lin, L., Hengzhi, Fu. (2005). Solidification Behaviour of Al-7%Si-Mg Casting Alloys. *Trans. Nonferrous Met. Soc.China*, 15, 1.